Accepted Manuscript

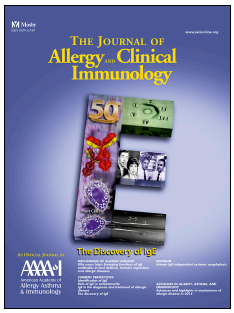

Mesenchymal stem cells alleviate oxidative stress-induced mitochondrial dysfunction in the airways

Xiang Li, PhD, Charalambos Michaeloudes, PhD, Yuelin Zhang, PhD, Coen H. Wiegman, PhD, Ian M. Adcock, PhD, Qizhou Lian, PhD, Judith C.W. Mak, PhD, Pankaj K. Bhavsar, PhD, Kian Fan Chung, MD

PII: S0091-6749(17)31431-8

DOI: 10.1016/j.jaci.2017.08.017

Reference: YMAI 12998

To appear in: *Journal of Allergy and Clinical Immunology*

Received Date: 30 September 2016

Revised Date: 7 July 2017

Accepted Date: 23 August 2017

Please cite this article as: Li X, Michaeloudes C, Zhang Y, Wiegman CH, Adcock IM, Lian Q, Mak JCW, Bhavsar PK, Chung KF, Mesenchymal stem cells alleviate oxidative stress-induced mitochondrial dysfunction in the airways, *Journal of Allergy and Clinical Immunology* (2017), doi: 10.1016/j.jaci.2017.08.017.

Mesenchymal stem cells alleviate oxidative stress-induced mitochondrial dysfunction in the airways

Xiang Li, PhD[1,2*], Charalambos Michaeloudes, PhD[1*], Yuelin Zhang, PhD[2,3*,] Coen H. Wiegman, PhD[1], Ian M. Adcock PhD[1], , Qizhou Lian, PhD[2,3,5], Judith C.W. Mak, PhD[2,4,5], Pankaj K. Bhavsar, PhD[1#], Kian Fan Chung, MD[1]

[1]National Heart and Lung Institute, Imperial College London, London, United Kingdom; Departments of Medicine[2], Ophthalmology[3] and Pharmacology & Pharmacy[4]; Shenzhen Institute of Research and Innovation[5], The University of Hong Kong, Hong Kong SAR

*These authors contributed equally to this study.

Corresponding author: Dr. Pankaj K Bhavsar[#], National Heart & Lung Institute, Dovehouse Street, London, SW3 6LY, United Kingdom. Tel: +44 20 7594 7961. Fax: +44 20 351 8126. Email: p.bhavsar@imperial.ac.uk.

Co-Corresponding authors: Dr Qizhou Lian, Departments of Medicine, and Ophthalmology and Shenzhen Institute of Research and Innovation, The University of Hong Kong, Hong Kong SAR, Email: qzlian@hku.hk

Dr Judith C.W. Mak, Departments of Medicine and Pharmacology and Pharmacy, and Shenzhen Institute of Research and Innovation, The University of Hong Kong, Hong Kong SAR. Email: judymak@hku.hk

This study was supported by project grants from Imperial College Trust, from National Natural Science Fund of China (NSFC No. 81370140 to JCW Mak; STFGD No.2015B020225001; RGC/GRF No. HKU17113816 and NSFC No. 31571407 to Q Lian) and by Respiratory Disease Biomedical Research Unit at the Royal Brompton NHS Foundation Trust and Imperial College London. KFC is a Senior Investigator of NIHR, UK.

ABSTRACT

Background: Oxidative stress-induced mitochondrial dysfunction may contribute to inflammation and remodeling in chronic obstructive pulmonary disease (COPD). Mesenchymal stem cells (MSCs) protect against lung damage in animal models of COPD. It is unknown whether these effects occur through attenuating mitochondrial dysfunction in airway cells.

Objective: To examine the effect of induced-pluripotent stem cell-derived MSCs (iPSC-MSCs) on oxidative stress-induce mitochondrial dysfunction in human airway smooth muscle cells (ASMCs) *in vitro* and in mouse lungs *in vivo*.

Methods: ASMCs were co-cultured with iPSC-MSCs in the presence of cigarette smoke medium (CSM), and mitochondrial reactive oxygen species (ROS), mitochondrial membrane potential ($\Delta\Psi m$) and apoptosis were measured. Conditioned media from iPSC-MSCs and trans-well co-cultures were used to detect any paracrine effects. The effect of systemic injection of iPSC-MSCs on airway inflammation and hyper-responsiveness in ozone-exposed mice was also investigated.

Results: Co-culture of iPSC-MSCs with ASMCs attenuated CSM-induced mitochondrial ROS, apoptosis and $\Delta\Psi m$ loss in ASMCs. iPSC-MSC-conditioned media or trans-well co-cultures with iPSC-MSCs reduced CSM-induced mitochondrial ROS but not $\Delta\Psi m$ or apoptosis in ASMCs. Mitochondrial transfer from iPSC-MSCs to ASMCs was observed after direct co-culture and was enhanced by CSM. iPSC-MSCs attenuated ozone-induced mitochondrial dysfunction, airway hyper-responsiveness and inflammation in mouse lungs.

Conclusion: iPSC-MSCs offered protection against oxidative stress-induced mitochondrial dysfunction in human ASMCs and in mouse lungs, whilst reducing airway inflammation and hyper-responsiveness. These effects are, at least partly, dependent on cell-cell contact that allows for mitochondrial transfer, and paracrine regulation. Therefore, iPSC-MSCs show promise as a therapy for oxidative stress-dependent lung diseases such as COPD.

(250 words)

KEY MESSAGES:

- Induced-pluripotent stem cell-derived mesenchymal stem cells (iPSC-MSCs) protect against cigarette smoke medium (CSM)-induced mitochondrial dysfunction and apoptosis in airway smooth muscle cells (ASMCs).
- The protective effect of iPSC-MSCs against CSM-induced mitochondrial dysfunction may be exerted through mitochondrial transfer and paracrine effects. iPSC-MSCs prevent mitochondrial dysfunction, airway hyper-responsiveness and inflammation in an ozone-induced mouse model of COPD highlighting the potential of these cells as a novel cell-based therapy.

CAPSULE SUMMARY:

iPSC-MSCs protect against oxidative stress-induced mitochondrial dysfunction, apoptosis, hyper-responsiveness and inflammation in the airways. These findings highlight the potential use of iPSC-MScs as a novel cell-based therapy for COPD.

KEYWORDS (up to 10)

Mesenchymal stem cell, chronic obstructive pulmonary disease, oxidative stress, airway smooth muscle, mitochondria, cigarette smoke, ozone, airway hyper-responsiveness, apoptosis, inflammation.

ABBREVIATIONS

AHR: airway hyper-responsiveness

ASMC: airway smooth muscle cell

BAL: bronchoalveolar lavage

BM-MSC: bone marrow mesenchymal stem cell

CdM: conditioned medium

COPD: chronic obstructive pulmonary disease

CS: cigarette smoke

CSM: cigarette smoke medium

DCF-DA: dichlorofluorescein diacetate

iPSC-MSC: induced-pluripotent stem cell-derived mesenchymal stem cells

JC-1: 5,5',6,6'-Tetrachloro-1,1',3,3'-tetraethylbenzimidazolylcarbocyanineiodide

-logPC100: concentration of acetylcholine that increased lung resistance by 100%

$\Delta\Psi m$: mitochondrial membrane potential

MSC: mesenchymal stem cells

R_L: pulmonary resistance

ROS: reactive oxygen species

TNT: tunneling nanotube

TUNEL: terminal deoxynucleotidyltransferase-mediated dUTP nick end labeling

INTRODUCTION

Chronic obstructive pulmonary disease (COPD) is a progressive airway inflammatory disease characterized by persistent airflow obstruction with poor reversibility usually caused by cigarette smoking (1). COPD is predicted to become the fourth leading cause of death globally by 2030 (2). The characteristic pathological features of COPD include a chronic inflammatory response and airway remodeling of the small airways with fibrosis and airway smooth muscle (ASM) thickening, together with emphysema (3). In addition to their contractile properties, ASM cells (ASMCs) have the potential to release pro-inflammatory mediators and growth factors (4-6). Oxidative stress resulting from persistent exposure to reactive oxygen species (ROS) and impaired anti-oxidant protection, is a key player underlying the pathogenesis of COPD (4). Cigarette smoke (CS) is a major source of ROS and the effects of oxidative stress can persist even after smoking cessation in patients with COPD (7), indicating that endogenous ROS resulting from the ensuing inflammatory response may also contribute to the development of oxidative stress.

Mitochondria are a major intracellular source of ROS (8). Defective oxidative phosphorylation in damaged mitochondria may lead to enhanced mitochondrial ROS production (8). In addition, loss of mitochondrial membrane potential ($\Delta\Psi m$) is regarded as an early event in the induction of mitochondrial apoptosis (9). Recently, mitochondrial dysfunction has been reported in the airways and lungs of patients with COPD (10-13), and has been shown to contribute to airway inflammation and remodelling in *in vivo* models of COPD (10, 14, 15). Defective mitochondrial

function, featuring reduced mitochondrial respiration and ATP production, has been reported in ASMCs from COPD patients (10). These observations indicate that mitochondria may be a promising therapeutic target for COPD.

Mesenchymal stem cells (MSCs) have shown promise as a potential cell-based therapy for COPD. MSCs display anti-inflammatory effects and attenuate alveolar destruction in animal models of COPD (16, 17), although the underlying mechanisms remain unresolved. We have reported that the protective effects of induced-pluripotent stem cell-derived MSCs (iPSC-MSCs), a novel type of MSCs, in a CS-induced rat model of COPD are accompanied by mitochondrial transfer from iPSC-MSCs to airway cells (18). However, the effect of MSCs on mitochondrial dysfunction remains unknown.

In this study we hypothesized that iPSC-MSCs can attenuate oxidative stress-induced mitochondrial dysfunction in human primary ASMCs and in an oxidant-induced mouse model (19-22). The effect of direct co-culture with iPSC-MSCs on CS-induced mitochondrial ROS, $\Delta\Psi m$ loss and induction of apoptosis in ASMCs was investigated. Mitochondrial transfer from iPSC-MSCs to ASMCs was also determined. The paracrine effects of iPSC-MSCs on ASMCs were investigated by using iPSC-MSC-conditioned media (CdM) or a trans-well co-culture system. Finally, we studied the effect of systemic delivery of iPSC-MSCs on mitochondrial function, airway inflammation and airway hyper-responsiveness (AHR) in an ozone-induced mouse model.

METHODS

Detailed descriptions of methods are listed in the *Online Repository*.

Primary human ASMCs and human iPSC-MSCs

ASMCs were isolated from endobronchial biopsies, or tracheas of healthy transplant donor lungs and cultured as previously described (23). Human iPSC-MSCs from a single donor were derived using a previously published protocol (24).

Direct co-culture

CSM was prepared as previously described (25). In a prophylactic protocol, $1x10^5$ASMCs were stained with CellTrace Violet and cultured with $1.5x10^5$ unstained iPSC-MSCs for 20 hours followed by CSM (10% or 25%) treatment for 4 hours. Alternatively, in a therapeutic protocol, $1x10^5$ ASMCs were stained with CellTrace Violet and treated with CSM. After 4 hours, CSM was removed and $1.5x10^5$ iPSC-MSCs were added to the culture for 24 hours.

Treatment of ASMCs with iPSC-MSC-conditioned media

Supernatants from iPSC-MSC cultures were concentrated 20-fold to create conditioned medium (CdM), as previously described (26). ASMCs were pretreated with 20-fold diluted CdM for 4 hours and then treated with CSM (10% or 25%) for 4 hours.

Transwell co-culture

$1x10^5$ ASMCs were grown at the bottom of 6-well culture plates and $1.5x10^5$ iPSC-MSCs were grown on cell-culture plate inserts with a pore-size of 0.4 μm. Cells were co-cultured for 20 hours and then treated with CSM for 4 hours.

Ozone-exposed mouse model

Male C57BL/6 mice were exposed to ozone (3 ppm in air) for 3 hours as previously reported (19-22). $1x10^6$ iPSC-MSCs were intravenously injected 24 hours prior to, or 6 hours after, the exposure. 21 hours post-exposure, AHR was measured and lungs were collected for analysis.

Isolation of intact mitochondria from mouse lungs

Intact mitochondria were isolated from mouse lungs using a Mitochondria Isolation Kit for Tissue (Thermo Fisher Scientific) according to the manufacturer's instructions.

Assessment of mitochondrial function and apoptosis

Cells or intact mitochondria were incubated with 5 μM MitoSOX Red, 2 μM JC-1(5,5',6,6'-Tetrachloro-1,1',3,3'-tetraethylbenzimidazolylcarbocyanineiodide) or 20-fold diluted FITC-conjugated Annexin V to determine changes in mitochondrial ROS, $\Delta\Psi m$ or apoptosis, respectively. ROS levels in cytoplasmic fractions of mouse lung extracts were determined by dichlorofluorescein diacetate (DCF-DA; 10μM) staining.

Detection of mitochondrial transfer in co-culture

CellTrace-labelled ASMCs and MitoTracker-labelled iPSC-MSCs were cultured together for 20 hours and then treated with CSM for 4 hours. The percentage of MitoTracker-positive ASMCs was measured by flow cytometry. Alternatively, the co-cultured cells were fixed, stained with Alexa Fluor 488-conjugated phalloidin and mitochondrial transfer was visualized by fluorescence microscopy.

188 **Airways hyper-responsiveness (AHR) measurement and bronchoalveolar lavage**
189 **(BAL) cell counts**

190 Measurement of AHR, and total and differential BAL cell counts were performed as
191 previously reported (20).

192 **Detection of apoptosis in mouse lungs**

193 Apoptosis in lung sections was detected using Terminal deoxynucleotidyl transferase
194 dUTP nick end labelling (TUNEL) staining using the In Situ Cell Death Detection Kit
195 (Roche, Mannheim, Germany). Positive cell numbers of 5 random fields for each
196 slide were counted.

197 **Statistical analysis**

198 Data are presented as mean ± standard error of mean (SEM). Statistical analysis was
199 performed using the Prism 5.0 software (Graphpad, San Diego, CA). Comparisons in
200 the *in vitro* study were carried out using a repeated measures one-way ANOVA
201 followed by Bonferroni post-hoc test. In the *in vivo* study comparisons were carried
202 out using the Kruskal-Wallis test followed by the Mann-Whitney test for pair-wise
203 comparisons. p-value < 0.05 was considered as statistically significant.

204

205

RESULTS

Effect of direct co-culture with iPSC-MSCs on CSM-induced mitochondrial dysfunction and apoptosis in ASMCs

In a prophylactic protocol, iPSC-MSCs were directly co-cultured with CellTrace-labelled ASMCs for 20 hours and then treated with CSM (10 and 25%) for 4 hours. ASMCs were identified as CellTrace-positive and iPSC-MSCs as CellTrace-negative cells using flow cytometry (Figure 1A).

Mitochondrial ROS levels were measured in the gated ASMC (CellTrace-positive) population and compared with the ASMCs in the single-culture. CSM increased the levels of mitochondrial ROS in ASMCs in single culture in a concentration-dependent manner (Figure 1B), an effect partially-prevented by co-culture with iPSC-MSCs (Figure 1B). In the therapeutic protocol, CellTrace-labelled ASMCs were treated with CSM for 4 hours before iPSC-MSCs were added to the culture and incubated for a further 20 hours. Under these conditions only 25% CSM led to a significant increase in mitochondrial ROS (Figure 1C). A small but significant reduction in mitochondrial ROS was observed in the ASMCS of co-culture group compared to the single culture treated with 25% CSM (Figure 1C).

In the prophylactic experiment, CSM induced a concentration-dependent reduction in $\Delta\Psi m$ in single cultures of ASMCs (Figure 1D). Co-culture with iPSC-MSCs prevented the reduction in $\Delta\Psi m$ induced by both 10% and 25% CSM treatment (Figure 1D). In the therapeutic experiment, 20 hours after removal of CSM, single-cultures of ASMCs continued to show significantly reduced $\Delta\Psi m$ in both the

10% and the 25% CSM-treated group (Figure 1E). In contrast, CSM did not significantly reduce ΔΨm in ASMCs co-cultured with iPSC-MSCs (Figure 1E).

Observing that iPSC-MSCs were more effective in attenuating CSM-induced mitochondrial dysfunction under the prophylactic protocol, we used this protocol to study the effect of co-culture on ASMC apoptosis. CSM increased the percentage of single-cultured ASMCs at 25% and 50% CSM (Figure 1F). In the absence of stimulation, iPSC-MSCs significantly increased the percentage of apoptotic ASMCs compared to those in the single-culture (Figure 1F). However, iPSC-MSCs led to a significant reduction in apoptosis induced by 25% and 50% CSM indicating that direct interaction with iPSC-MSCs can protect ASMCs from CSM-induced apoptosis (Figure 1F).

Paracrine effects of iPSC-MSCs on CSM-induced mitochondrial dysfunction and apoptosis in ASMCs

We studied the contribution of paracrine mediators in the protective effects of iPSC-MSCs on CSM-induced ASMC mitochondrial dysfunction and apoptosis, by treating ASMCs with CdM from iPSC-MSCs or using trans-well co-culture. ASMCs treated with CdM demonstrated significantly lower levels of mitochondrial ROS in response to both 10% and 25% CSM (Figure 2A) compared to ASMCs cultured without CdM. However, CdM had no significant effect on CSM-mediated reduction in ΔΨm (Figure 2B) or induction of apoptosis (Figure 2C).

In line with the findings from the CdM experiments, ASMCs in trans-well co-culture with iPSC-MSCs demonstrated significantly lower levels of mitochondrial

ROS induced by 25% CSM compared to ASMCs (Figure 3A) compared to those cultured with blank inserts. However, no significant difference in ΔΨm (Figure 3B) and apoptosis (Figure 3C) was observed between the iPSC-MSCs treatment and blank insert.

Mitochondrial Transfer from iPSC-MSCs to ASMCs

To investigate mitochondrial transfer from iPSC-MSCs to ASMCs, ASMCs were pre-stained with CellTrace Violet, while iPSC-MSCs were pre-stained with the mitochondrial-targeted dye MitoTracker Red. Cells were co-cultured for 20 hours followed by 4 hours stimulation with 25% CSM, and further stained with phalloidin which selectively stains F-actin fibers. MitoTracker-labelled mitochondria were observed in CellTrace-labelled ASMCs, indicating transfer of mitochondria from iPSC-MSCs to ASMCs (Figure 4A). Tunneling nanotube (TNT)-like structures, containing iPSC-MSC mitochondria, were observed connecting iPSC-MSCs and ASMCs. Actin filaments were identified in the TNTs confirming a connection between the cytoskeletons of the two cell types (Figure 4A).

The percentage of MitoTracker-positive cells in the ASMC population was quantified using flow cytometry (Figure 4B). CSM elevated the mitochondrial transfer rate in a concentration-dependent manner (Figure 4C). Under similar experimental conditions, green fluorescence protein-tagged mitochondria from iPSC-MSCs were observed in TNT-like structures between iPSC-MSCs and ASMCs and, importantly, also in CellTrace-labelled ASMCs (Supplementary Figure E1), further confirming transfer of mitochondria from iPSC-MSCs to ASMCs in response

272 to CSM.

273

274 **Effect of iPSC-MSCs on ozone-induced cellular ROS, mitochondrial dysfunction**
275 **and apoptosis in mouse lungs**

276 The effects of iPSC-MSCs on mitochondrial function and apoptosis were studied in
277 mice acutely exposed to ozone. There were five treatment groups in this study:
278 Air/saline (n=5), Air with iPSC-MSCs administrated 24 hours prior-exposure
279 (Air/-24hr; n=5), Ozone/saline (n=6), Ozone with iPSC-MSCs administrated 24 hours
280 prior-exposure (Ozone/-24hr; n=6) and the Ozone with iPSC-MSCs administrated 6
281 hour post-exposure (Ozone/+6hr; n=6).

282 Ozone exposure significantly elevated the cytoplasmic ROS levels. No
283 significant effects were observed in either the Ozone/-24hr or the Ozone/+6hr group
284 in comparison with the Ozone/saline group (Figure 5A).

285 Mitochondrial ROS levels were significantly elevated in the Ozone/saline group
286 compared with the Air/Saline group (Figure 5B). Both the Ozone/-24hr and the
287 Ozone/+6hr group demonstrated significantly reduced mitochondrial ROS levels
288 compared to the Ozone/saline group. In addition, the mitochondrial ROS levels in the
289 Ozone/+6hr group were significantly lower than the Ozone/-24hr group (Figure 5B).

290 Exposure to ozone reduced the $\Delta\Psi m$ of isolated mitochondria in comparison to
291 the air/saline group (Figure 5C). The Ozone/-24hr showed an increase in $\Delta\Psi m$
292 compared with the Ozone/saline group. However, the Ozone/+6hr group did not show
293 a significant difference compared to the Ozone/saline group, and the $\Delta\Psi m$ was still

294 significantly lower than the Air/saline group.

295 Ozone exposure significantly increased the number of apoptotic cells in lung
296 sections in saline groups (Figure 6A-B). Both the Ozone/-24hr and the Ozone/+6hr
297 groups showed significantly reduced number of apoptotic cells compared with the
298 Ozone/saline group (Figure 6A-B).

299

300 **Effect of iPSC-MSCs on ozone-induced AHR and lung inflammation**

301 Pulmonary resistance (R_L) in response to increasing concentrations of
302 acetylcholine was measured 21 hours after exposure (Figure 7A). The Ozone/saline
303 group demonstrated significantly increased AHR compared with the Air/saline group
304 as shown by a reduction in $-\log PC_{100}$ (Figure 7B). The Ozone/-24hr group showed
305 significantly lower AHR compared to the Ozone/saline group (Figure 7B). The
306 Ozone/+6hr group, in contrast, did not exhibit a difference in AHR compared to the
307 Ozone/saline group (Figure 7B).

308 The ozone/saline group demonstrated significantly higher total cell numbers in
309 the BAL compared to the Air/saline group (Figure 7C), with increased number of
310 neutrophils (Figure 7D), macrophages (Figure 7E), eosinophils (Figure 7F) and
311 lymphocytes (Figure 7G). The total cell numbers in the Ozone/-24hr group were
312 significantly lower compared to Ozone/saline group whilst the Ozone/+6hr group did
313 not show any effect (Figure 7C). The Ozone/-24hr group showed significantly
314 reduced neutrophil numbers compared to the Ozone/saline group (Figure 7D) while
315 the Ozone/+6hr group did not show any effect. Macrophage, eosinophil and

316 lymphocyte numbers showed a decreasing trend in the Ozone/-24hr and/or the
317 Ozone/+6hr group which did not, however, reach statistical significance (Figures
318 7E-7G).

319 Thus, iPSC-MSCs were able to prevent but not reverse ozone-induced AHR and
320 recruitment of inflammatory cells into the lung.

321

322 **DISCUSSION**

323 We have shown that direct co-culture of ASMCs with iPSC-MSCs protected the
324 former from CSM-induced mitochondrial ROS production, mitochondrial
325 depolarization and apoptosis. When the ASMCs were exposed to supernatants from
326 iPSC-MSCs or trans-well inserts with iPSC-MSCs, only CSM-induced mitochondrial
327 ROS, but not mitochondrial depolarization and apoptosis in ASMCs were ameliorated,
328 indicating that soluble factors from iPSC-MSCs reduced the production of
329 mitochondrial ROS. When there was direct contact between iPSC-MSCs and ASMCs,
330 mitochondria were transferred from iPSC-MSCs to ASMCs, possibly through the
331 formation of tunneling nanotubes (TNTs), an effect that was enhanced by CSM
332 treatment. iPSC-MSCs were also able to prevent, but not reverse, ozone-induced
333 mitochondrial dysfunction, AHR and airway inflammation in a mouse model, an
334 effect likely to be a result of direct interaction and mitochondrial transfer between
335 iPSC-MSCs and airway cells.

336 Mesenchymal stem cells (MSCs) are fibroblast-like multipotent stem cells
337 residing in various tissues such as bone marrow and adipose tissue (27). The *in vitro*

differentiation of iPSCs into iPSC-MSCs provides a new source of MSCs. Compared to BM-MSCs, iPSC-MSCs were shown to have a higher proliferative and differentiation potential (24) and a superior capacity to attenuate CS-induced airway inflammation, apoptosis and emphysema in rats (18, 28). Here, we demonstrate for the first time, that iPSC-MSCs are capable of alleviating oxidative stress-induced mitochondrial dysfunction in lung cells. The therapeutic effects of iPSC-MSCs appear to be less pronounced than the prophylactic effects both *in vitro* and *in vivo*, possibly due to the progression of mitochondrial dysfunction to an irreversible stage, the partial recovery of mitochondrial function following the removal of CSM stimulation *in vitro*, or shorter length of treatment time of iPSC-MSCs *in vivo*.

Targeting mitochondrial dysfunction represents a novel strategy for developing treatments for COPD. Mitochondrial dysfunction has been demonstrated in ASMCs from patients with COPD, as characterized by a reduction in ATP levels, mitochondrial complex protein expression and membrane potential, as well as elevation in mitochondrial ROS (10). The mitochondrial-targeted antioxidant, MitoQ, was found to prevent mitochondrial dysfunction as well as airway inflammation and AHR in an ozone-induced mouse model, indicating that mitochondrial dysfunction may contribute to the development of disease pathology (10). CSM was reported to induce mitochondrial dysfunction involving increased mitochondrial fragmentation and ROS production and a reduction in mitochondrial respiration in airway epithelial cells (11) and ASMCs (29). Oxidative stress-induced mitochondrial dysfunction can further induce oxidative stress, leading to apoptosis (8, 9) which contributes to the

alveolar destruction in COPD (30). In the current study, we demonstrated that the alleviation of oxidative stress-induced mitochondrial dysfunction by iPSC-MSCs was accompanied by reduced apoptosis and airway inflammation and hyper-responsiveness in mice.

While MSCs have been reported to induce paracrine effects by releasing immune-regulatory cytokines (16), in the present study, CdM was only able to ameliorate CSM-induced mitochondrial ROS in ASMCs without any effect on $\Delta\Psi m$ or apoptosis. It is possible that the release of protective paracrine factors by iPSC-MSCs may be triggered by mediators produced by the damaged ASMCs. However, in a trans-well co-culture system where there is paracrine crosstalk between the two cell types the iPSC-MSCs also prevented CSM-induced mitochondrial ROS production but not the reduction of $\Delta\Psi m$ or apoptosis in ASMCs. Paracrine factors may therefore only partly contribute to the protective effects of iPSC-MSCs, and direct cell-cell contact is crucial for the full protective effects to take place.

Mitochondrial transfer was first identified in co-cultures of BM-MSCs and lung epithelial cells with defective mitochondria (31). Mitochondrial transfer from MSCs to epithelial cells was also observed *in vivo* in rodent models of acute lung injury (32) and CS-induced emphysema (18). In the current study we report mitochondrial transfer from iPSC-MSCs to ASMCs which is enhanced by CSM. A previous study reported that CS exposure can lead to a reduction in the supply of respiratory substrates to the electron transport chain in mouse lungs leading to increased bioenergetic demand (15). The transfer of iPSC-MSC-derived mitochondria may

enhance the bioenergetic capacity of ASMCs and thus prevent CSM-induced mitochondrial stress. In addition mitochondrial transfer may exert its effects indirectly by activating protective signalling pathways involved in the activation of antioxidant responses and/or mitochondrial biogenesis and quality control. Understanding these mechanisms will require further investigation.

We have observed formation of TNTs connecting the cytoskeletons of iPSC-MSCs and ASMCs. TNTs are highly sensitive nanotubular structures which facilitate the selective transfer of membrane-bound vesicles and organelles between cells (33). TNTs have been reported to mediate mitochondrial transfer from BM-MSCs to epithelial cells, from endothelial cells to cancer cells and from vascular smooth muscle cells to MSCs (31, 34, 35). Therefore, the transfer of mitochondria from iPSC-MSCs to ASMCs may occur via TNTs. Recent studies have demonstrated that the mitochondrial Rho-GTPase Miro1 facilitates mitochondrial movement through the TNTs (36, 37). The mechanisms driving TNT formation and/or mitochondrial movement between iPSC-MSCs and ASMCs in response to oxidative stress will be investigated in the future.

Despite the reduction in ozone-induced mitochondrial ROS by iPSC-MSCs, ozone-induced cytoplasmic ROS levels were not modulated by iPSC-MSCs. These results suggest that instead of a general anti-oxidant effect, the protective action of iPSC-MSCs may be through specifically restoring mitochondrial dysfunction. This might explain why antioxidants such as N-acetylcysteine that do not target mitochondria have not had much clinical success in the treatment of COPD (38).

There are several limitations to this study. Firstly, in the absence of CSM treatment, the co-culture with iPSC-MSCs increased the apoptosis of ASMCs, suggesting that iPSC-MSCs may induce stress in the target cells at baseline. Such data imply that the safety of iPSC-MSCs should be carefully examined. Moreover, although we used *in vitro* and *in vivo* models of oxidative stress-induced mitochondrial dysfunction these do not represent the situation in COPD lungs. Therapeutic potential of iPSC-MSCs in COPD can be further confirmed by studying ASMCs from COPD patients, in which mitochondria are known to be already impaired (10). We have chosen to study the effect of iPSC-MSCs on ASMCs as these cells were shown to have impaired mitochondrial function in COPD (10), and are known to play a key role in the development of airway remodelling and inflammation (4, 39). However, it would be crucial to determine the efficacy of iPSC-MSCs on other airway cell types such as epithelial cells and fibroblasts in order to gain a better understanding of the potential of iPSC-MSCs as cell-based therapy for lung disease. Secondly, an additional limitation could include our use of cigarette smoke medium prepared using Marlboro Red cigarettes instead of using research cigarettes which are produced to provide standardized amounts of components in the cigarette smoke. However, although we used commercial cigarettes, the effects of cigarette smoke medium on mitochondrial function and apoptosis were very consistent between experiments despite using primary cells that have an inherent variability in their responses. In order to minimise further the variability in the cigarette smoke medium preparations, we used a peristaltic pump to bubble the cigarette smoke into the

medium at a constant speed. Thirdly, , TNTs are not only involved in mitochondrial transfer but may also facilitate the exchange of other cellular organelles or molecules that may protect the ASMCs from mitochondrial dysfunction. Finally, a drawback of using fluorescent dyes to study mitochondrial transfer is that any dye leaking out from dead iPSC-MSCs may be taken up by ASMCs, leading to false-positive results. We have addressed this by expressing fluorescence-labelled mitochondria in iPSC-MSCs. These data confirm mitochondrial transfer, through TNT, from iPSC-MSC to ASMC in response to stimulation with CSM.

In summary, we have shown that the capacity of iPSC-MSCs to attenuate oxidative stress-induced mitochondrial dysfunction and to protect against lung damage and inflammation relies on direct cell-cell contact that allows mitochondrial transfer. We conclude that iPSC-MSCs are effective in protecting against oxidative stress-induced mitochondrial dysfunction in the lungs and are thus a promising candidate for development of cell-based therapies in COPD.

ACKNOWLEDGMENTS

We would like the thank Dr Han Shuo and Dr Liang Yingmin for their contribution to the performing the studies described in the supplementary data.

References

1. Barnes PJ. Chronic obstructive pulmonary disease. *N Engl J Med* 2000; 343: 269-280.

2. Mathers CD, Loncar D. Projections of global mortality and burden of disease from 2002 to 2030. *PLoS Med* 2006; 3: e442.

3. Hogg JC, Chu F, Utokaparch S, Woods R, Elliott WM, Buzatu L, Cherniack RM, Rogers RM, Sciurba FC, Coxson HO, Pare PD. The nature of small-airway obstruction in chronic obstructive pulmonary disease. *N Engl J Med* 2004; 350: 2645-2653.

4. Chung KF, Adcock IM. Multifaceted mechanisms in COPD: inflammation, immunity, and tissue repair and destruction. *Eur Respir J* 2008; 31: 1334-1356.

5. Jarai G, Sukkar M, Garrett S, Duroudier N, Westwick J, Adcock I, Chung KF. Effects of interleukin-1beta, interleukin-13 and transforming growth factor-beta on gene expression in human airway smooth muscle using gene microarrays. *Eur J Pharmacol* 2004; 497: 255-265.

6. Howarth PH, Knox AJ, Amrani Y, Tliba O, Panettieri RA, Jr., Johnson M. Synthetic responses in airway smooth muscle. *J Allergy Clin Immunol* 2004; 114: S32-50.

7. Louhelainen N, Rytila P, Haahtela T, Kinnula VL, Djukanovic R. Persistence of oxidant and protease burden in the airways after smoking cessation. *BMC pulmonary medicine* 2009; 9: 25.

8. Marchi S, Giorgi C, Suski JM, Agnoletto C, Bononi A, Bonora M, De Marchi E, Missiroli S, Patergnani S, Poletti F, Rimessi A, Duszynski J, Wieckowski MR, Pinton P. Mitochondria-ros crosstalk in the control of cell death and aging. *J Signal Transduct* 2012; 2012: 329635.

9. Green DR, Reed JC. Mitochondria and apoptosis. *Science* 1998; 281: 1309-1312.

10. Wiegman CH, Michaeloudes C, Haji G, Narang P, Clarke CJ, Russell KE, Bao W, Pavlidis S, Barnes PJ, Kanerva J, Bittner A, Rao N, Murphy MP, Kirkham PA, Chung KF, Adcock IM, Copdmap. Oxidative stress-induced mitochondrial dysfunction drives inflammation and airway smooth muscle remodeling in patients with chronic obstructive pulmonary disease. *J Allergy Clin Immunol* 2015; 136: 769-780.

11. Hoffmann RF, Zarrintan S, Brandenburg SM, Kol A, de Bruin HG, Jafari S, Dijk F, Kalicharan D, Kelders M, Gosker HR, Ten Hacken NH, van der Want JJ, van Oosterhout AJ, Heijink IH. Prolonged cigarette smoke exposure alters mitochondrial structure and function in airway epithelial cells. *Respir Res* 2013; 14: 97.

12. Ahmad T, Sundar IK, Lerner CA, Gerloff J, Tormos AM, Yao H, Rahman I. Impaired mitophagy leads to cigarette smoke stress-induced cellular senescence: implications for chronic obstructive pulmonary disease. *FASEB J* 2015; 29: 2912-2929.

13. Mizumura K, Cloonan SM, Nakahira K, Bhashyam AR, Cervo M, Kitada T, Glass K, Owen CA, Mahmood A, Washko GR, Hashimoto S, Ryter SW, Choi AM.

494 Mitophagy-dependent necroptosis contributes to the pathogenesis of COPD. *J*
495 *Clin Invest* 2014; 124: 3987-4003.
496 14. Cloonan SM, Glass K, Laucho-Contreras ME, Bhashyam AR, Cervo M, Pabon
497 MA, Konrad C, Polverino F, Siempos, II, Perez E, Mizumura K, Ghosh MC,
498 Parameswaran H, Williams NC, Rooney KT, Chen ZH, Goldklang MP, Yuan
499 GC, Moore SC, Demeo DL, Rouault TA, D'Armiento JM, Schon EA,
500 Manfredi G, Quackenbush J, Mahmood A, Silverman EK, Owen CA, Choi
501 AM. Mitochondrial iron chelation ameliorates cigarette smoke-induced
502 bronchitis and emphysema in mice. *Nat Med* 2016; 22: 163-174.
503 15. Agarwal AR, Zhao L, Sancheti H, Sundar IK, Rahman I, Cadenas E. Short-term
504 cigarette smoke exposure induces reversible changes in energy metabolism
505 and cellular redox status independent of inflammatory responses in mouse
506 lungs. *Am J Physiol Lung Cell Mol Physiol* 2012; 303: L889-898.
507 16. Weiss DJ, Bertoncello I, Borok Z, Kim C, Panoskaltsis-Mortari A, Reynolds S,
508 Rojas M, Stripp B, Warburton D, Prockop DJ. Stem cells and cell therapies in
509 lung biology and lung diseases. *Proc Am Thorac Soc* 2011; 8: 223-272.
510 17. Weiss DJ. Concise review: current status of stem cells and regenerative medicine
511 in lung biology and diseases. *Stem Cells* 2014; 32: 16-25.
512 18. Li X, Zhang Y, Yeung SC, Liang Y, Liang X, Ding Y, Ip MS, Tse HF, Mak JC,
513 Lian Q. Mitochondrial transfer of induced pluripotent stem cell-derived
514 mesenchymal stem cells to airway epithelial cells attenuates cigarette
515 smoke-induced damage. *Am J Respir Cell Mol Biol* 2014; 51: 455-465.

19. Cho HY, Zhang LY, Kleeberger SR. Ozone-induced lung inflammation and hyperreactivity are mediated via tumor necrosis factor-alpha receptors. *Am J Physiol Lung Cell Mol Physiol* 2001; 280: L537-546.

20. Wiegman CH, Li F, Clarke CJ, Jazrawi E, Kirkham P, Barnes PJ, Adcock IM, Chung KF. A comprehensive analysis of oxidative stress in the ozone-induced lung inflammation mouse model. *Clin Sci (Lond)* 2014; 126: 425-440.

21. Triantaphyllopoulos K, Hussain F, Pinart M, Zhang M, Li F, Adcock I, Kirkham P, Zhu J, Chung KF. A model of chronic inflammation and pulmonary emphysema after multiple ozone exposures in mice. *Am J Physiol Lung Cell Mol Physiol* 2011; 300: L691-700.

22. Williams AS, Issa R, Leung SY, Nath P, Ferguson GD, Bennett BL, Adcock IM, Chung KF. Attenuation of ozone-induced airway inflammation and hyper-responsiveness by c-Jun NH2 terminal kinase inhibitor SP600125. *J Pharmacol Exp Ther* 2007; 322: 351-359.

23. Michaeloudes C, Sukkar MB, Khorasani NM, Bhavsar PK, Chung KF. TGF-beta regulates Nox4, MnSOD and catalase expression, and IL-6 release in airway smooth muscle cells. *Am J Physiol Lung Cell Mol Physiol* 2011; 300: L295-304.

24. Lian Q, Zhang Y, Zhang J, Zhang HK, Wu X, Lam FF, Kang S, Xia JC, Lai WH, Au KW, Chow YY, Siu CW, Lee CN, Tse HF. Functional mesenchymal stem cells derived from human induced pluripotent stem cells attenuate limb ischemia in mice. *Circulation* 2010; 121: 1113-1123.

538 25. Lau WK, Chan SC, Law AC, Ip MS, Mak JC. The role of MAPK and Nrf2
539 pathways in ketanserin-elicited attenuation of cigarette smoke-induced IL-8
540 production in human bronchial epithelial cells. *Toxicol Sci* 2012; 125:
541 569-577.
542 26. Zhang Y, Liao S, Yang M, Liang X, Poon MW, Wong CY, Wang J, Zhou Z,
543 Cheong SK, Lee CN, Tse HF, Lian Q. Improved cell survival and paracrine
544 capacity of human embryonic stem cell-derived mesenchymal stem cells
545 promote therapeutic potential for pulmonary arterial hypertension. *Cell*
546 *Transplant* 2012; 21: 2225-2239.
547 27. Teo AK, Vallier L. Emerging use of stem cells in regenerative medicine. *The*
548 *Biochemical journal* 2010; 428: 11-23.
549 28. Li X, Zhang Y, Liang Y, Cui Y, Yeung SC, Ip MS, Tse HF, Lian Q, Mak JC.
550 iPSC-derived mesenchymal stem cells exert SCF-dependent recovery of
551 cigarette smoke-induced apoptosis/proliferation imbalance in airway cells. *J*
552 *Cell Mol Med* 2016.
553 29. Aravamudan B, Kiel A, Freeman M, Delmotte P, Thompson M, Vassallo R, Sieck
554 GC, Pabelick CM, Prakash YS. Cigarette smoke-induced mitochondrial
555 fragmentation and dysfunction in human airway smooth muscle. *Am J Physiol*
556 *Lung Cell Mol Physiol* 2014; 306: L840-854.
557 30. Demedts IK, Demoor T, Bracke KR, Joos GF, Brusselle GG. Role of apoptosis in
558 the pathogenesis of COPD and pulmonary emphysema. *Respir Res* 2006; 7:
559 53.

560 31. Spees JL, Olson SD, Whitney MJ, Prockop DJ. Mitochondrial transfer between
561 cells can rescue aerobic respiration. *Proc Natl Acad Sci U S A* 2006; 103:
562 1283-1288.
563 32. Islam MN, Das SR, Emin MT, Wei M, Sun L, Westphalen K, Rowlands DJ,
564 Quadri SK, Bhattacharya S, Bhattacharya J. Mitochondrial transfer from
565 bone-marrow-derived stromal cells to pulmonary alveoli protects against acute
566 lung injury. *Nat Med* 2012; 18: 759-765.
567 33. Rustom A, Saffrich R, Markovic I, Walther P, Gerdes HH. Nanotubular highways
568 for intercellular organelle transport. *Science* 2004; 303: 1007-1010.
569 34. Vallabhaneni KC, Haller H, Dumler I. Vascular smooth muscle cells initiate
570 proliferation of mesenchymal stem cells by mitochondrial transfer via
571 tunneling nanotubes. *Stem Cells Dev* 2012; 21: 3104-3113.
572 35. Pasquier J, Guerrouahen BS, Al Thawadi H, Ghiabi P, Maleki M, Abu-Kaoud N,
573 Jacob A, Mirshahi M, Galas L, Rafii S, Le Foll F, Rafii A. Preferential transfer
574 of mitochondria from endothelial to cancer cells through tunneling nanotubes
575 modulates chemoresistance. *J Transl Med* 2013; 11: 94.
576 36. Ahmad T, Mukherjee S, Pattnaik B, Kumar M, Singh S, Kumar M, Rehman R,
577 Tiwari BK, Jha KA, Barhanpurkar AP, Wani MR, Roy SS, Mabalirajan U,
578 Ghosh B, Agrawal A. Miro1 regulates intercellular mitochondrial transport &
579 enhances mesenchymal stem cell rescue efficacy. *EMBO J* 2014; 33:
580 994-1010.
581 37. Zhang Y, Yu Z, Jiang D, Liang X, Liao S, Zhang Z, Yue W, Li X, Chiu SM, Chai

582 YH, Liang Y, Chow Y, Han S, Xu A, Tse HF, Lian Q. iPSC-MSCs with High
583 Intrinsic MIRO1 and Sensitivity to TNF-alpha Yield Efficacious
584 Mitochondrial Transfer to Rescue Anthracycline-Induced Cardiomyopathy.
585 *Stem Cell Reports* 2016; 7: 749-763.
586 38. Johnson K, McEvoy CE, Naqvi S, Wendt C, Reilkoff RA, Kunisaki KM,
587 Wetherbee EE, Nelson D, Tirouvanziam R, Niewoehner DE. High-dose oral
588 N-acetylcysteine fails to improve respiratory health status in patients with
589 chronic obstructive pulmonary disease and chronic bronchitis: a randomized,
590 placebo-controlled trial. *Int J Chron Obstruct Pulmon Dis* 2016; 11: 799-807.
591 39. Chung KF. The role of airway smooth muscle in the pathogenesis of airway wall
592 remodeling in chronic obstructive pulmonary disease. *Proc Am Thorac Soc*
593 2005; 2: 347-354; discussion 371-342.
594
595

FIGURE LEGENDS

Figure 1. Effects of direct co-culture with iPSC-MSCs on mitochondrial dysfunction and apoptosis in ASMCs. (A) Detection of ASMCs (CellTrace-positive) and iPSC-MSCs (CellTrace-negative) in the co-culture by flow cytometry. (B-C) Prophylactic (B; n=7) and therapeutic (C; n=6) effects of direct-co-culture with iPSC-MSCs on CSM (10-25%; 4 hours)-dependent mitochondrial ROS production in ASMCs. (D-E) Prophylactic (D; n=5) and therapeutic (E; n=3) effects of iPSC-MSCs on CSM (10-25%; 4 hours)-dependent ΔΨm in ASMCs. (F) Prophylactic effects of iPSC-MSCs on CSM-(10-50%; 4 hours)-dependent apoptosis in ASMCs. *p<0.05, **p<0.01, ***p<0.001. Mean ± SEM are shown.

Figure 2. Effects of CdM from iPSC-MSCs on mitochondrial dysfunction and apoptosis in ASMCs. Effect of 4 hour pre-treatment with iPSC-MSC-derived CdM on CSM (10-25%; 4 hours)-dependent mitochondrial ROS (A; n=6), ΔΨm (B; n=4) and apoptosis (C; n=4). *p<0.05, **p<0.01, ***p<0.001. Mean ± SEM are shown.

Figure 3. Effects of co-culture with iPSC-MSCs in trans-well inserts on mitochondrial dysfunction and apoptosis in ASMCs. Effect of co-culture of ASMCs with iPSC-MSCs using a trans-well culture system for 20 hours on CSM (10-25%; 4 hours)-dependent mitochondrial ROS (A; n=4), ΔΨm (B; n=4) and apoptosis (C; n=4) in ASMCs. *p<0.05, **p<0.01, ***p<0.001. Mean ± SEM are shown.

Figure 4. Mitochondrial transfer from iPSC-MSCs to ASMCs. (A) Visualisation of TNT formation and mitochondrial transfer in iPSC-MSCs (MitoTracker-stained) and ASMCs (CellTrace-stained) co-cultures using fluorescence microscopy. Scale bar=25 μm. (B) Mitochondrial transfer from iPSC-MSCs (MitoTracker-positive) to ASMCs (CellTrace-positive) was determined by flow cytometry. The gate indicates the ASMC population. (C) The rate of mitochondrial transfer was evaluated by the percentage of MitoTracker-positive ASMCs in the total ASMC population (n=3). *p<0.05, ***p<0.001. Mean ± SEM are shown.

Figure 5. Effects of iPSC-MSCs on ozone-induced ROS and mitochondrial dysfunction in mouse lungs. Effect of prophylactic (24 hours prior to exposure; -24hr) and therapeutic (6 hours post-exposure; +6hr) intravenous administration of iPSC-MSCs on cytoplasmic ROS (A), mitochondrial ROS (B) and ΔΨm in the lungs of mice exposed to ozone (3ppm) for 3 hours. *p<0.05, **p<0.01 compared to air/saline; #p<0.05 compared to air/-24hr, $^{\dagger}p$<0.05, $^{\dagger\dagger}p$<0.01 compared to ozone/saline; $^{\S\S}p$<0.01 compared to ozone/-24hr. Mean ± SEM are shown.

Figure 6. Effects of iPSC-MSCs on ozone-induced apoptosis in mouse lungs. Effect of prophylactic (24 hours prior to exposure; -24hr) and therapeutic (6 hours post-exposure; +6hr) intravenous administration of iPSC-MSCs on the number of apoptotic (TUNEL-positive) cells in lung sections of mice exposed to ozone (3ppm)

for 3 hours. Cell nuclei were visualized using DAPI staining (A). Apoptotic cells were counted in five randomly selected 20x fields for each mouse using a fluorescent microscope (B). Scale bar=50μm. *p<0.05 compared to air/saline; $^{\dagger\dagger}p$<0.01 compares to ozone/saline. Mean ± SEM are shown.

Figure 7. Effects of iPSC-MSCs on ozone-induced AHR and airway inflammation. Effect of prophylactic (24 hours prior to exposure; -24hr) and therapeutic (6 hours post-exposure; +6hr) intravenous administration of iPSC-MSCs on R_L in response to increasing concentration of acetylcholine (A), -log PC_{100} (B) total BAL cell number (C), neutrophil number (D), macrophage number (E), eosinophil number (F) and lymphocyte number (G) . *p<0.05, **p<0.01 compared to air/saline; #p<0.05, ##p<0.01 compared to air/-24hr, $^{\dagger}p$<0.05, $^{\dagger\dagger}p$<0.01 compared to ozone/saline. Mean ± SEM are shown.

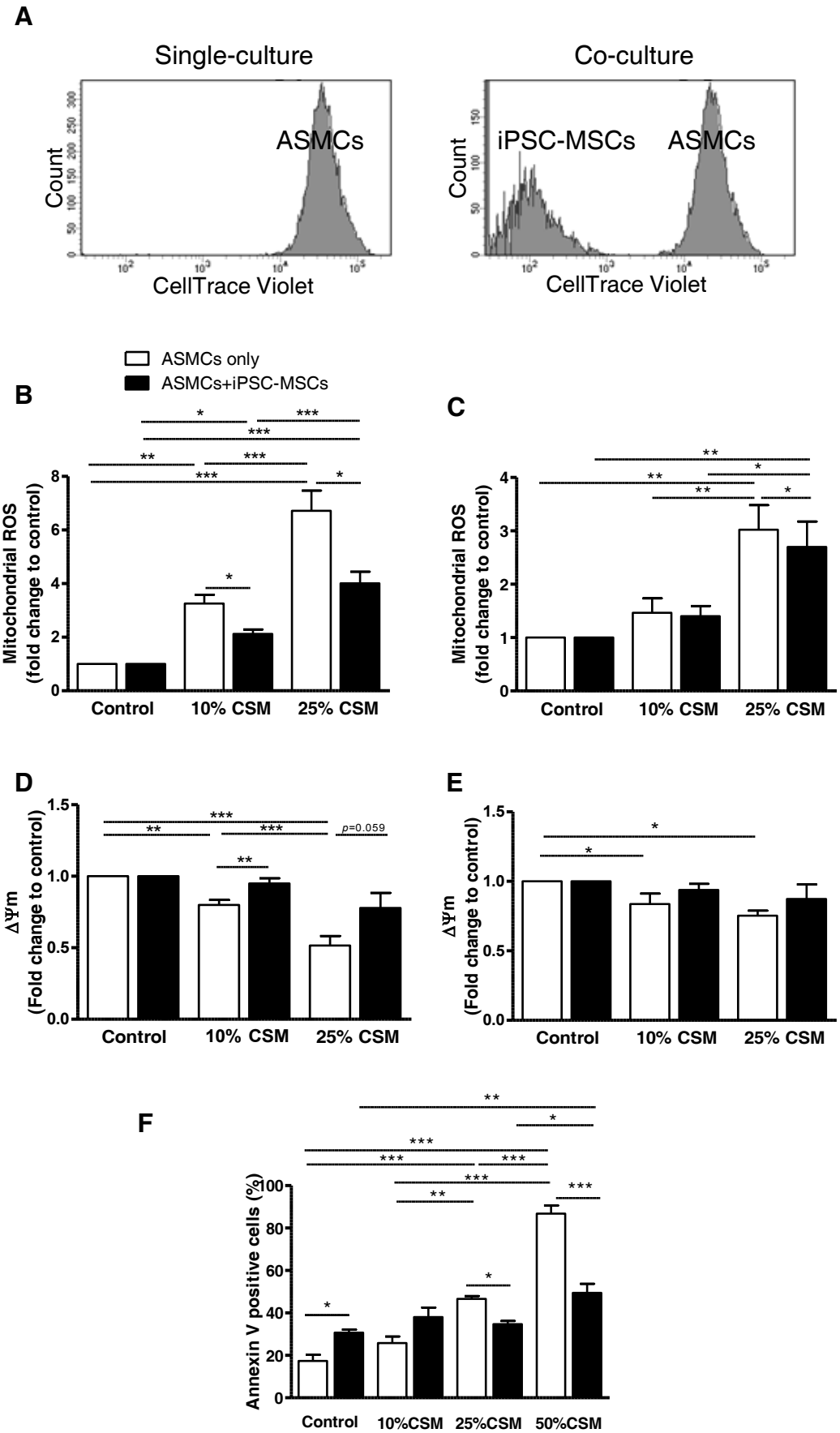
A
Single-culture
Co-culture
ASMCs
iPSC-MSCs
ASMCs
Count
CellTrace Violet
ASMCs only
ASMCs+iPSC-MSCs
B
C
Mitochondrial ROS
(fold change to control)
Control
10% CSM
25% CSM
D
E
ΔΨm
(Fold change to control)
p=0.059
F
Annexin V positive cells (%)
Control
10%CSM
25%CSM
50%CSM

Figure 1

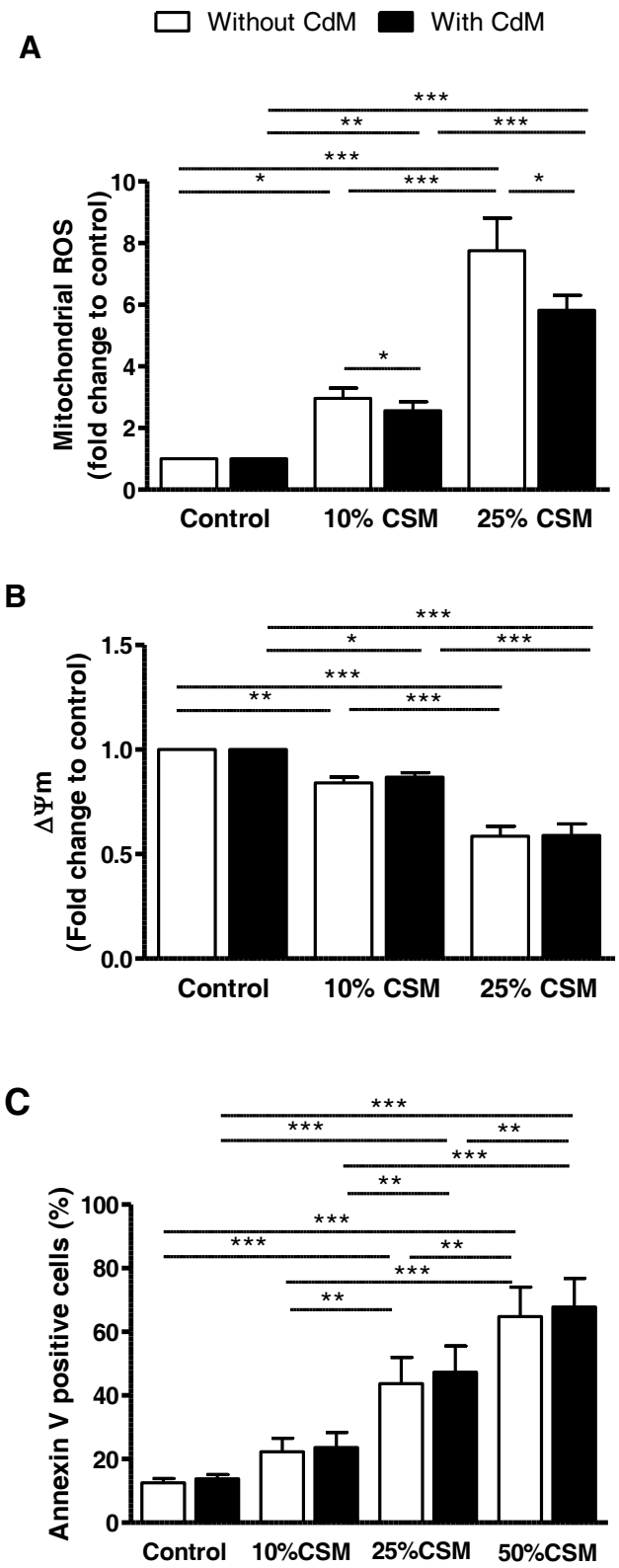
Without CdM
With CdM
A
Mitochondrial ROS
(fold change to control)
Control
10% CSM
25% CSM
B
ΔΨm
(Fold change to control)
Control
10% CSM
25% CSM
C
Annexin V positive cells (%)
Control
10%CSM
25%CSM
50%CSM

Figure 2

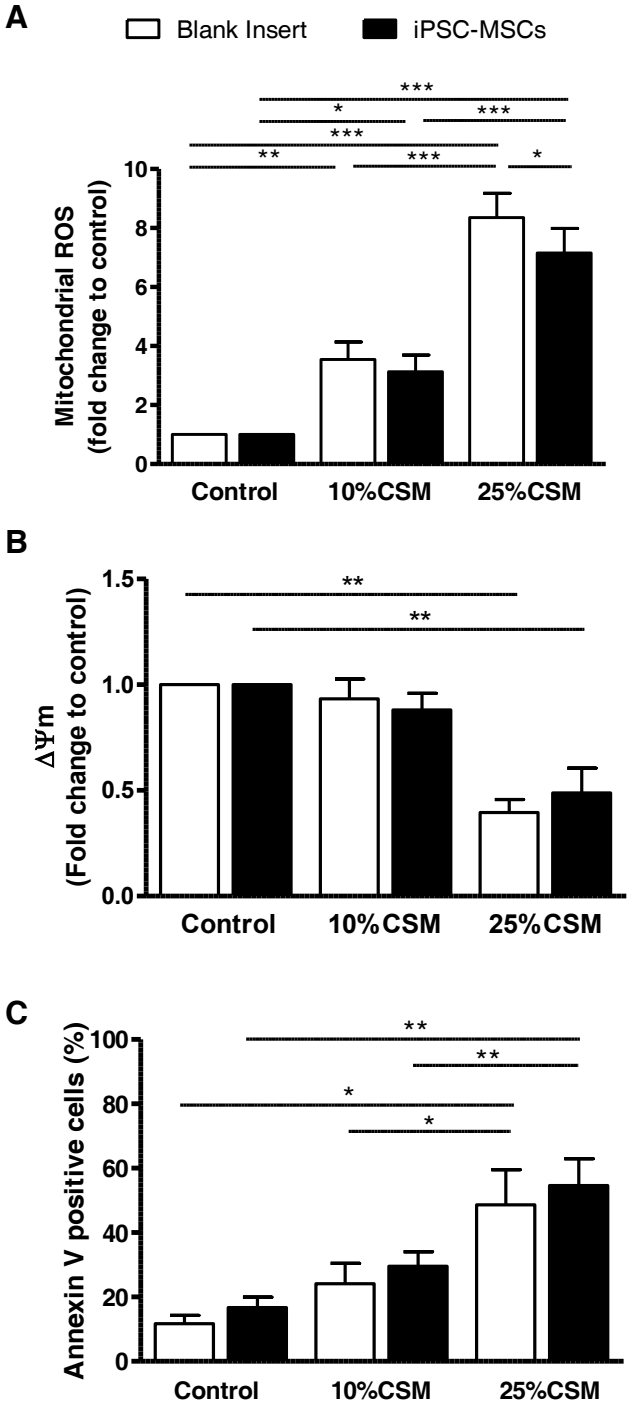
A
Blank Insert
iPSC-MSCs
Mitochondrial ROS
(fold change to control)
Control
10%CSM
25%CSM
B
ΔΨm
(Fold change to control)
Control
10%CSM
25%CSM
C
Annexin V positive cells (%)
Control
10%CSM
25%CSM

Figure 3

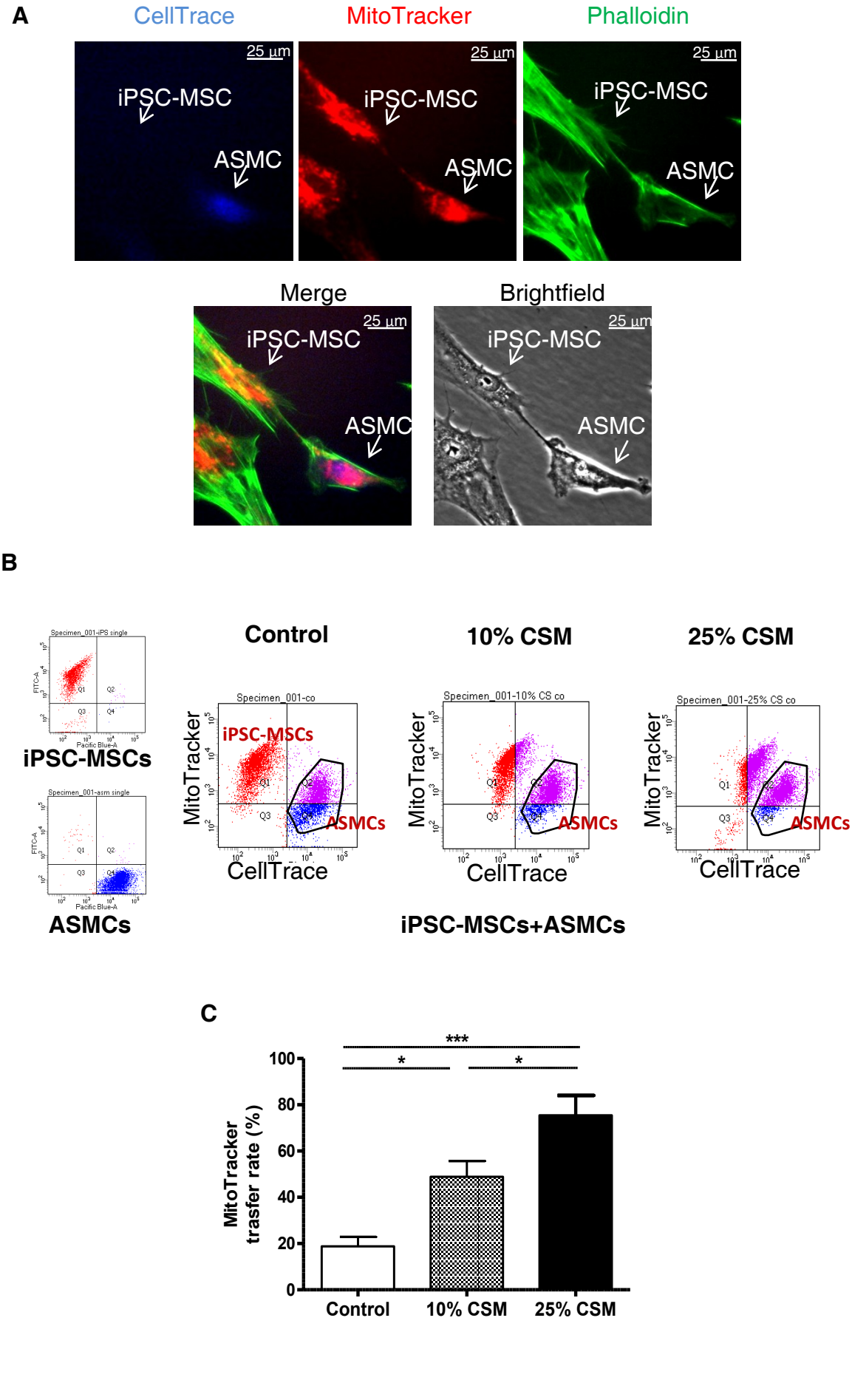
A
CellTrace
MitoTracker
Phalloidin
25 μm
iPSC-MSC
ASMC
Merge
Brightfield
B
Control
10% CSM
25% CSM
iPSC-MSCs
ASMCs
iPSC-MSCs+ASMCs
MitoTracker
CellTrace
C
MitoTracker trasfer rate (%)
Control
10% CSM
25% CSM

Figure 4

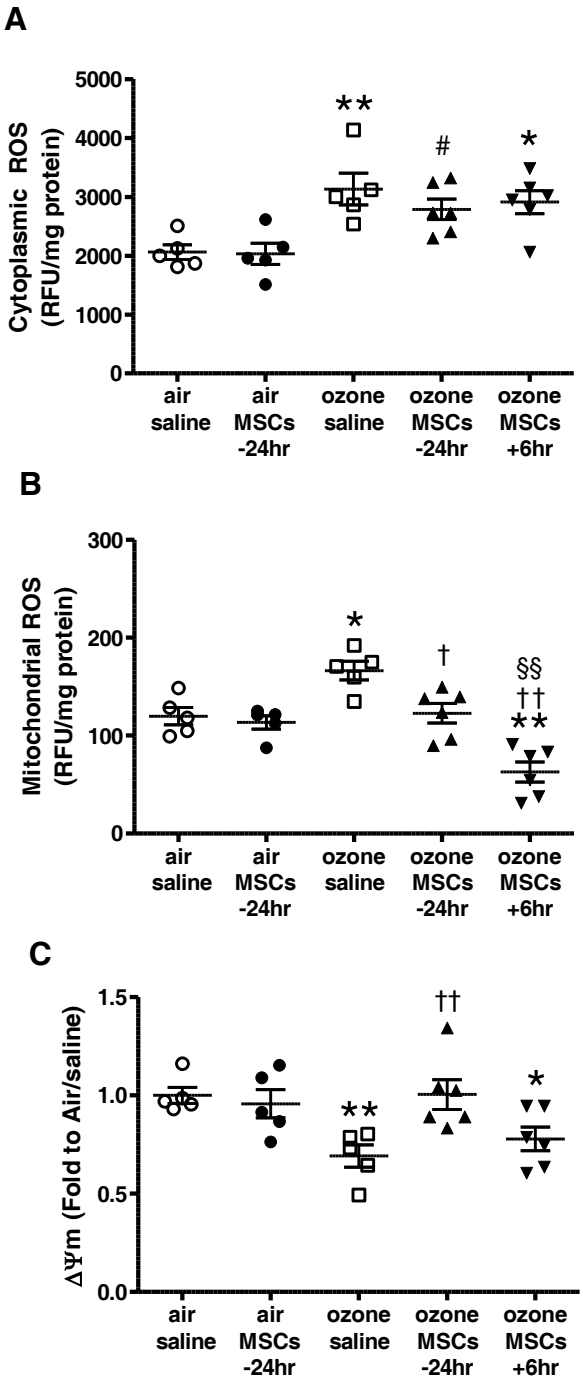
A
Cytoplasmic ROS (RFU/mg protein)
5000
4000
3000
2000
1000
0
**
#
*
air saline
air MSCs -24hr
ozone saline
ozone MSCs -24hr
ozone MSCs +6hr
B
Mitochondrial ROS (RFU/mg protein)
300
200
100
0
*
†
§§
††
**
air saline
air MSCs -24hr
ozone saline
ozone MSCs -24hr
ozone MSCs +6hr
C
ΔΨm (Fold to Air/saline)
1.5
1.0
0.5
0.0
**
††
*
air saline
air MSCs -24hr
ozone saline
ozone MSCs -24hr
ozone MSCs +6hr

Figure 5

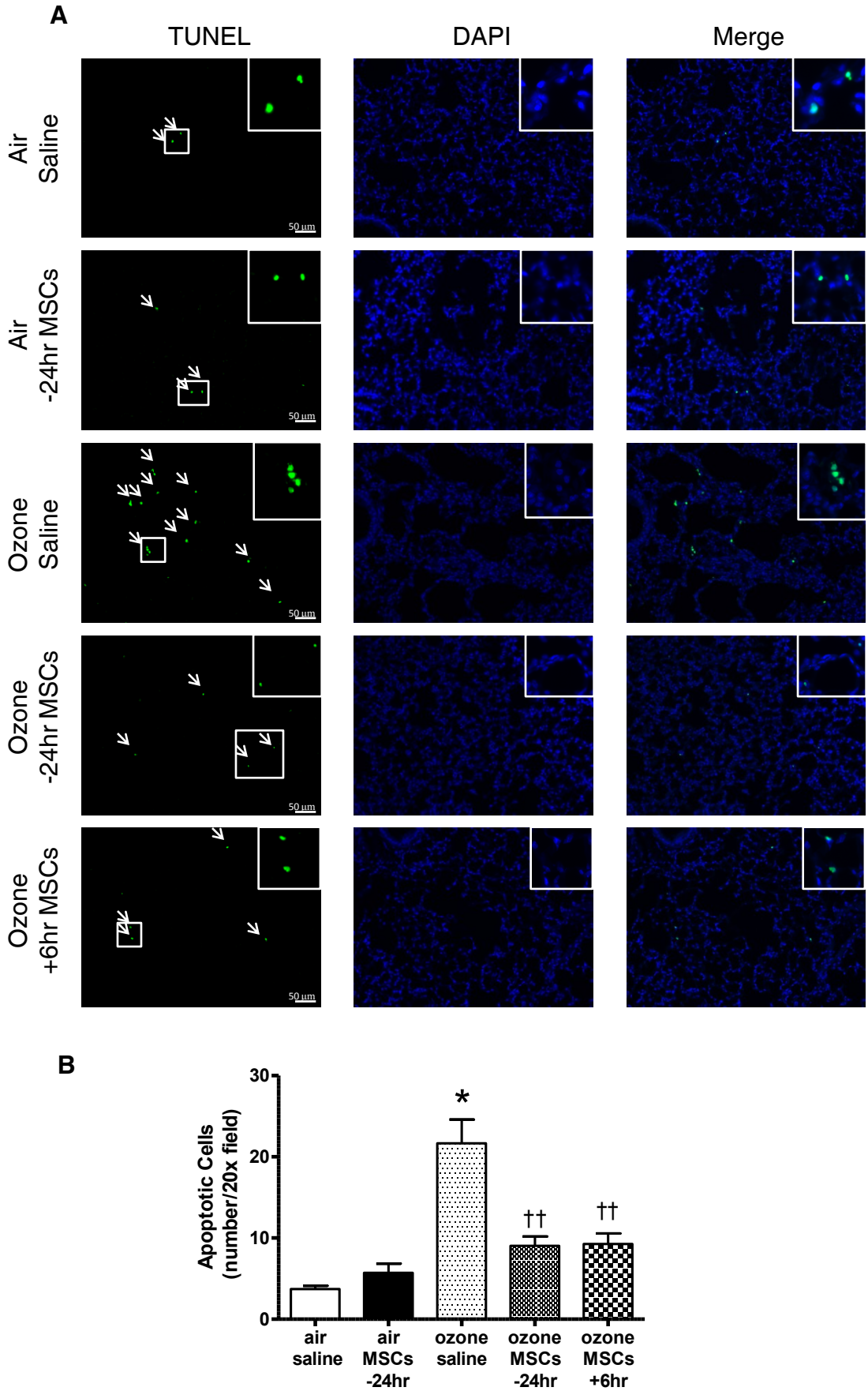
A
TUNEL
DAPI
Merge
Air Saline
Air -24hr MSCs
Ozone Saline
Ozone -24hr MSCs
Ozone +6hr MSCs
50 μm
B
Apoptotic Cells (number/20x field)
30
20
10
0
*
††
††
air saline
air MSCs -24hr
ozone saline
ozone MSCs -24hr
ozone MSCs +6hr

Figure 6

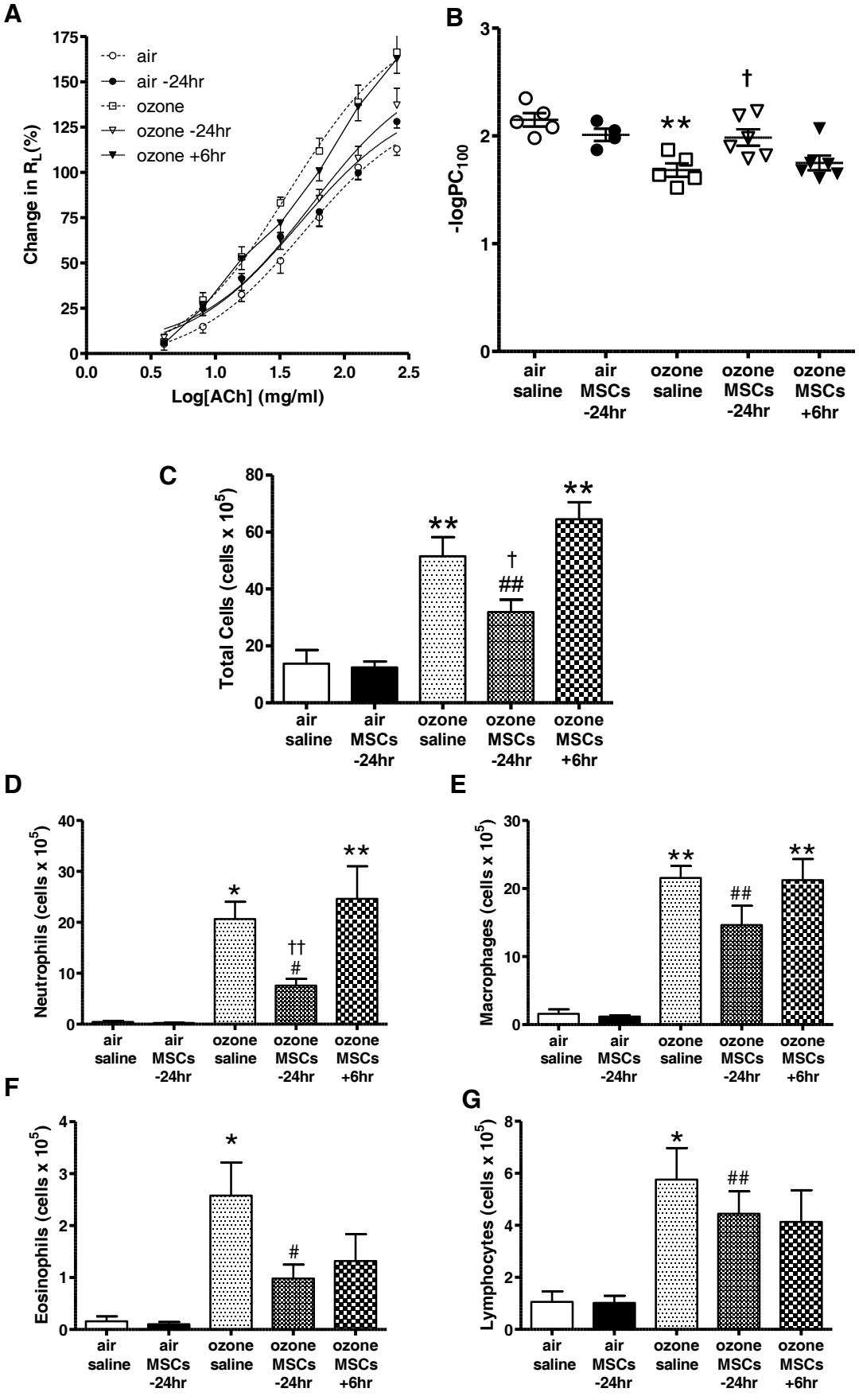
A
Change in R_L(%)
Log[ACh] (mg/ml)
air
air -24hr
ozone
ozone -24hr
ozone +6hr
B
-logPC100
C
Total Cells (cells x 10^5)
D
Neutrophils (cells x 10^5)
E
Macrophages (cells x 10^5)
F
Eosinophils (cells x 10^5)
G
Lymphocytes (cells x 10^5)
air saline
air MSCs -24hr
ozone saline
ozone MSCs -24hr
ozone MSCs +6hr

Figure 7

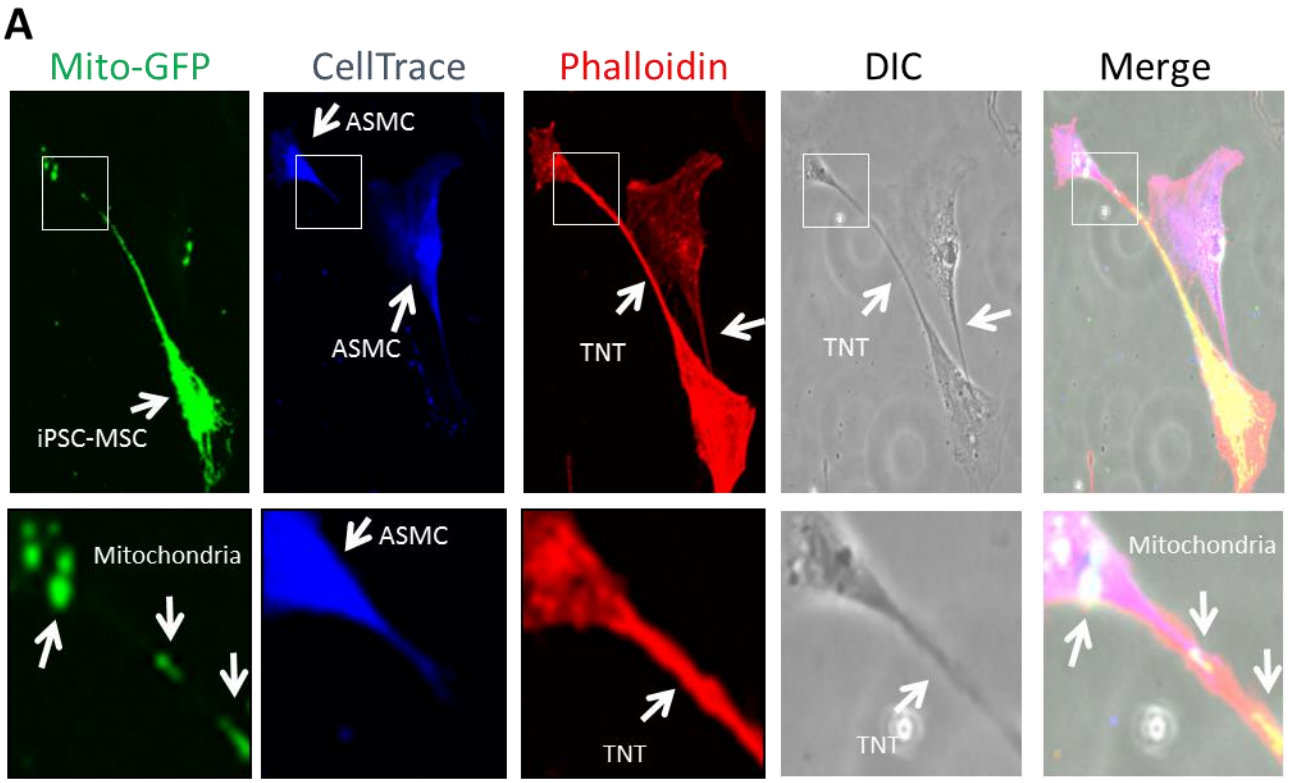
A
Mito-GFP
CellTrace
Phalloidin
DIC
Merge
ASMC
ASMC
iPSC-MSC
TNT
TNT
Mitochondria
ASMC
TNT
TNT
Mitochondria

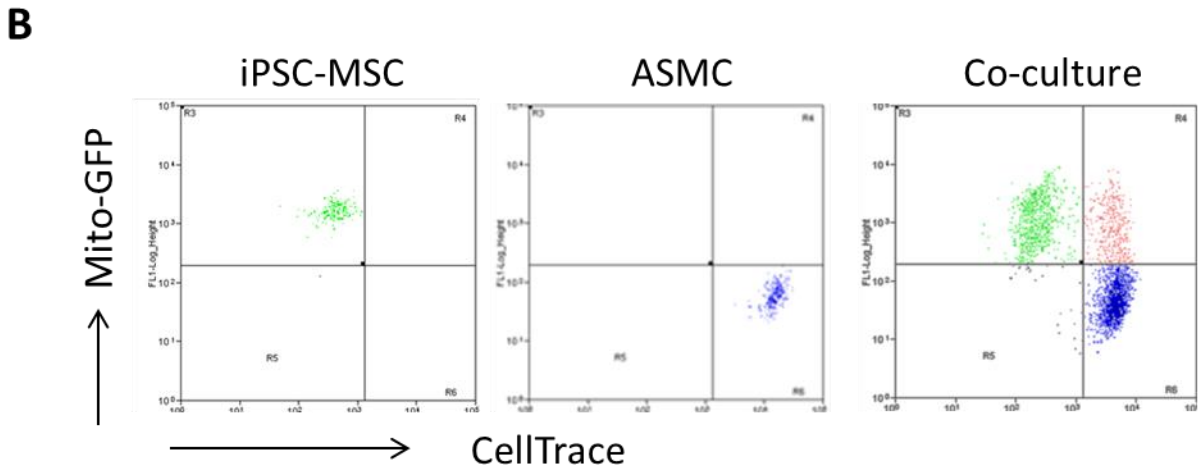
B
iPSC-MSC
ASMC
Co-culture
Mito-GFP
CellTrace

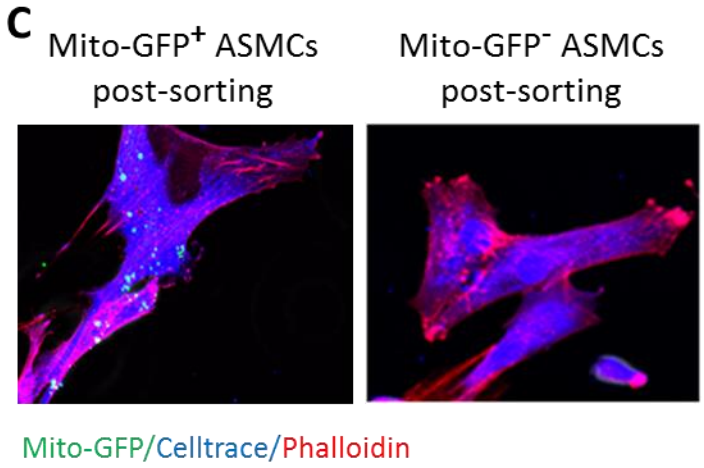
C
Mito-GFP+ ASMCs post-sorting
Mito-GFP- ASMCs post-sorting
Mito-GFP/Celltrace/Phalloidin

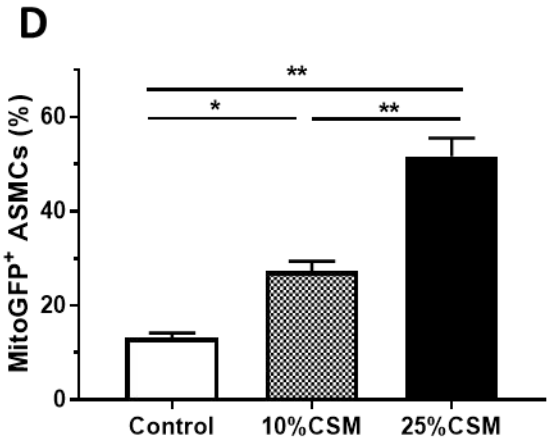
D
MitoGFP+ ASMCs (%)
0
20
40
60
**
*
**
Control
10%CSM
25%CSM

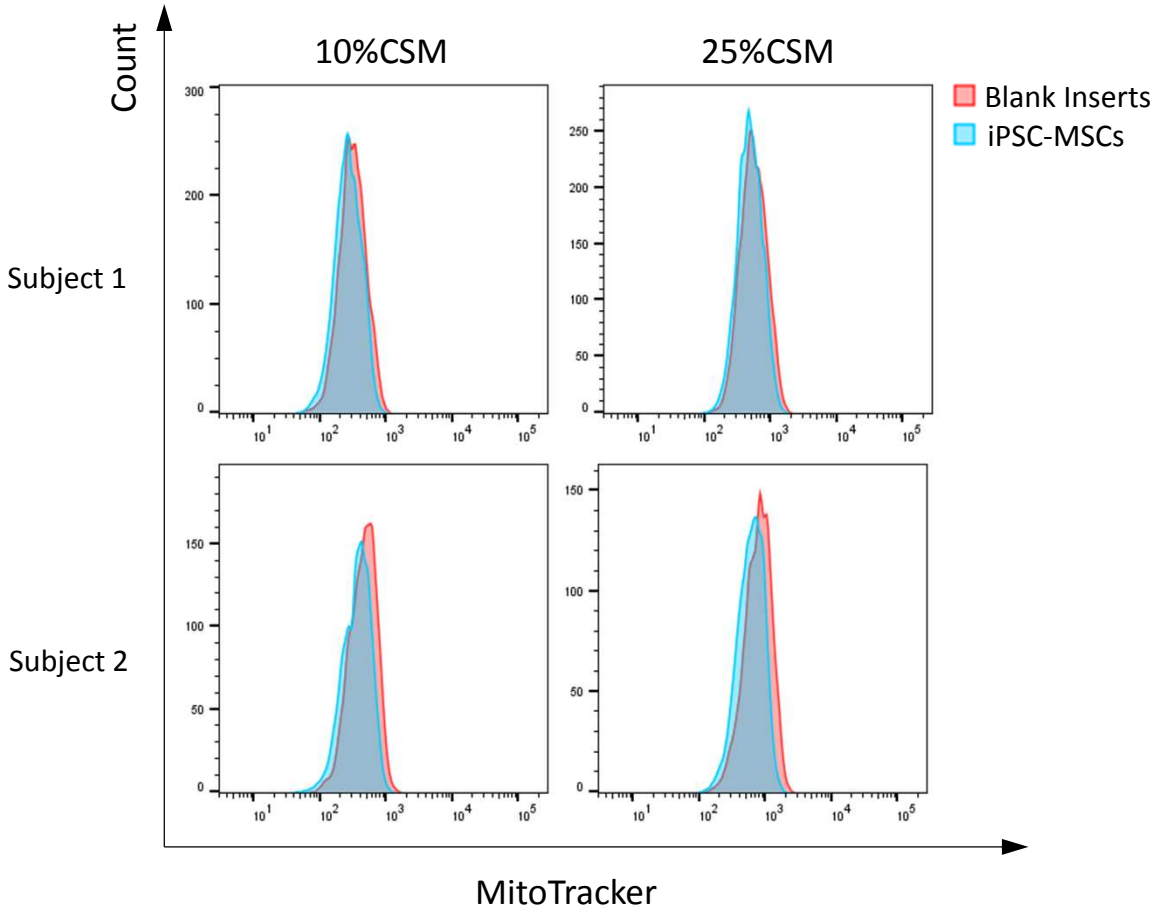

Figure S2. Quantification of leakage-induced MitoTracker staining on ASMCs

Li et al:Online Supplemental Data

Figure E1: Detection of mitochondrial transfer from Mito-GFP-iPSC-MSCs to ASMCs

Method

To avoid the leakage of MitoTracker from iPSC-MSCs to contaminate ASMCs, iPSC-MSCs were transfected with mitochondrial targeting green fluorescence protein (mito-GFP; pCT-MITO-GFP, Cat: Cyto102-PA-1, System Biosciences) by using lentiviral mediated transfection as previously described (Stem Cell Reports. 2016 Oct 11; 7(4): 749–763). Subsequently, CellTrace-labelled ASMCs and Mito-GFP-iPSC-MSCs were co-cultured for 20 hours and then treated with CSM (10%, 25%) for 4 hours, respectively. After treatment, the co-cultured cells were stained with Fulor-594-conjugated phalloidin and then mitochondrial transfer from Mito-GFP-iPSC-MSCs to ASMCs was examined by fluorescence microscopy. Furthermore, the percentage of Mito-GFP-positive ASMCs was evaluated by FACS. Sorted Mito-GFP^{+} and Mito-GFP^{-} AMSCs were further examined by fluorescent microscopy to confirm the Mito-GFP-mitochondria in the cells.

Result

Mito-GFP-iPSC-MSCs were co-cultured with CellTrace-labeled ASMCs for 20 hours and then exposed to CSM (10%, 25%) challenge. After 4 hour-treatment, phalloidin staining showed that tunneling nanotubes (TNT) were formed between iPSC-MSCs and ASMCs, allowing the mitochondrial transfer from MSCs to ASMCs (Fig. E1A). Importantly, some Mito-GFP mitochondria were observed in the middle of the TNT (Fig. E1A). The mitochondrial transfer

from Mito-iPSC-MSCs to ASMCs was also detected by FACS (Fig. E1B). The data show some CellTrace–labelled ASMCs were also positive for GFP, suggesting that mitochondria were transferred from MSCs to ASMCs (Fig. E1B). Moreover, compared with 10% CSM stimulation, more effective mitochondrial transfer from Mito-GFP-iPSC-MSCs to ASMCs was detected after 25% CSM stimulation (Fig. E1D, $p<0.01$). Finally, to verify the successful mitochondrial transfer, the Mito-GFP$^+$ ASMCs and Mito-GFP$^-$ ASMCs were isolated and then stained with phalloidin. Fluorescent microscopy showed that Mito-GFP mitochondria was only observed in Mito-GFP$^+$ ASMCs but not Mito-GFP$^-$ ASMCs (Fig. E1C).

Figure legend

(A) Representative images showing TNT formation and mitochondrial transfer between Mito-GFP-iPSC-MSCs and CellTrace-labeled ASMCs. Phalloidin staining shows F-actin fibers in TNTs. (B) Representative distribution of Mito-GFP-iPSC-MSCs and CellTrace-labeled ASMCs in co-cultured cells analyzed by FACS. (C) Representative images of mito-GFP$^+$ and mito-GFP$^-$ ASMCs sorted from the co-culture, demonstrating Mito-GFP-mitochondria only in the former population. (D) Percentage of Mito-GFP$^+$ ASMCs to the total ASMCs in the co-culture as an indication of mitochondrial transfer efficiency under different treatments (n=3). *$p<0.05$, **$p<0.01$. Mean ± SEM are shown.

Figure E2: Quantification of leakage-induced MitoTracker staining on ASMCs.

Method

To address this specific concern we have performed a trans-well culture experiment to test the possibility that MitoTracker released from dead or dying iPSC-MSCs may be taken up by ASMCs under our experimental conditions leading to false positive results. Specifically, ASMCs pre-stained with CellTrace were seeded in 6-well plates. Transwell inserts (pore size 0.4 µm) containing MitoTracker-labeled iPSC-MSCs or no cells were put into the 6-well plates for 20 hours followed by a 4-hour treatment of CSM.

Result

The results showed that there was no detectable uptake of MitoTracker dye by possible release from iPSC-MSCs (Figure E2). These data, importantly, clearly show that the increase in MitoTracker staining in ASMCs, under our co-culture conditions, is as a result of active mitochondrial transfer which is unlikely to be influenced by leakage of dye from iPSC-MSCs.

Figure Legend

CellTrace-labelled ASMCs were seeded in the wells of 6-well tissue culture plates, and MitoTracker-labelled iPSC-MSCs were seeded in inserts. ASMCs and iPSC-MSCs were co-cultured for 20 hrs and then incubated with CSM (10% or 25%) for 4 hrs. ASMCs cultured with blank inserts and treated with CSM (10% or 25%) were used as controls. MitoTracker staining in ASMCs (CellTrace-positive) was detected by flow cytometry.

Online Repository Materials and Methods

Primary human airway smooth muscle cells

Airway smooth muscle cells (ASMCs) were isolated from biopsies of bronchi, or tracheas of healthy transplant donor lungs as previously described (1). Briefly, endobronchial biopsies were cut into small pieces (<1 mm^2) and placed in Dulbecco modified Eagle's medium (DMEM) supplemented with 10% FBS, 4 mM L-glutamine, 100 U/ml of penicillin, 100 μg/ml streptomycin, 2.5 μg/ml amphotericin B and 10% foetal bovine serum (FBS), at 37^0C, 5% CO_2 and humidified atmosphere, to allow attachment and growth of ASMCs. Alternatively, ASMCs were dissected from tracheal segments from healthy transplant donor lungs.

ASMCs were identified by the characteristic "hill and valley" morphology under light microscopy. Cell stocks were kept in 175 cm^2 flasks at 37^0C, 5% CO_2 and humidified atmosphere. Experiments were carried out on cells at passages 3 to 7. Cells were treated in serum-free medium which consisted of phenol-red free DMEM supplemented with 1 mM sodium pyruvate, 4 mM L-glutamine, 1:100 non-essential amino acids, 0.1% BSA, 100 U/ml penicillin, 100 μg/ml streptomycin and 2.5 μg/ml amphotericin B.

Human iPSC-MSCs

Human iPSC-MSCs were derived based on a previously published protocol (2). Briefly, IMR90 fibroblast cells (Cat# CCL-186, American Type Culture Collection, Manassas, VA, USA) were transduced with lentiviral vectors carrying human OCT4, SOX2, NANOG and LIN28 genes (Plasmid 16577-80, Addgene, Cambridge, MA,

USA) followed by incubation with ES culture medium on inactivated mouse embryonic fibroblast feeder for 20 days. Colonies with human embryonic stem cell morphology were identified as iPSCs. For induced-differentiation, iPSCs were incubated in Dulbecco modified Eagle's medium (DMEM, Gibco, Carlsbad, CA, USA) supplemented with 10% serum replacement medium (Gibco), 10 ng/mL basic fibroblast growth factor (bFGF, Gibco), 10 ng/mL platelet-derived growth factor AB (Peprotech, Rocky Hill, NH, USA), and 10 ng/mL epidermal growth factor (EGF, Peprotech). One week later, differentiating iPSCs were harvested, incubated with CD24-phycoerythrin and CD105-FITC (BD PharMingen, San Diego, CA, USA) and sorted using a fluorescence-activated cell sorter (FACS). The $CD24^{-}CD105^{+}$ cells were sub-cultured in 96-well culture plates to select wells containing a single cell. The clones from a single cell were serially re-seeded to obtain a confluent 175-cm^2 tissue culture flask. The iPSC-MSCs were examined for surface marker profile (CD44+, CD49a+ CD49e+, CD73+, CD105+, CD166+, CD34−, CD45−, and CD133−). In addition, the differentiation capacity was tested by efficient adipogenesis, osteogenesis and chondrogenesis. They were then frozen down for future experiments. The iPSC-MSCs were cultured in DMEM (Gibco) supplemented with 10% FBS (Gibco), bFGF (5 ng/mL), and EGF (10 ng/mL). Cells were maintained in a humidified 37°C incubator with 5% CO_2.

Cigarette smoke medium (CSM)

CSM was prepared as previously described (3). Briefly, cigarette smoke from two filter-removed Marlboro Red cigarettes (10 mg TAR and 0.8 mg nicotine) was bubbled into 20 ml of serum-free medium using a peristaltic pump. The medium was

then filtered through a 0.22 μm filter. The optical density (OD) of the solution at a wavelength of 320 nm was measured. 100% CSM solution was generated by adjusting the OD of the solution to 1.1 absorbance units by diluting in serum-free medium.

We are aware of the importance of consistency and reproducibility for cigarette smoke (CS)-related studies due to the complex chemical components in cigarette smoke. To this end, we have put effort into optimizing our preparation protocol to produce consistent and reproducible CSM. Specifically, we used a peristaltic pump instead of a syringe to bubble the CS into medium as used in many previous reports that used both commercial cigarettes [4-7] and research cigarettes [8], as we found that the application of a constant pumping speed significantly reduces the variability of the CSM extracts The optical density (OD) at 320 nm was used as the indication of concentration of CSM (OD_{320} = 1.1 was defined 100%). We also found that only small variabilities between preparations should be adjusted by dilution (e.g. OD_{320} = 1.2 or 1.3, adjusted to 1.1 by dilution and considered 100%). We discarded the CSM preparations if OD_{320} was higher than 1.5, and prepared a new batch with OD_{320} close to 1.1. The resulting CSM preparations showed consistent effects on mitochondrial function and apoptosis in our experiments.

Direct co-culture of ASMCs and iPSC-MSCs

Direct co-culture of ASMCs and iPSC-MSCs was carried out using a prophylactic or a therapeutic protocol.

For the prophylactic protocol, ASMCs were trypsinized, pelleted, re-suspended and counted. $1x10^6$ ASMCs were washed with HBSS and then incubated with CellTrace Violet solution (Invitrogen, Paisley, UK), diluted 1:1000 in HBSS, for 20 minutes. Following centrifugation, ASMCs were incubated with complete medium for

10 minutes to wash and neutralize the dye. CellTrace-labelled ASMCs were mixed with the unstained iPSC-MSCs and seeded in 6-well culture plates at densities of $1x10^5$ ASMCs and $1.5x10^5$ iPSC-MSCs per well. Wells containing only $1x10^5$ ASMCs were used as controls (single culture control). After 20 hours, the medium was replaced with CSM (10-50%) for 4 hours before the cells were harvested for analysis.

For the therapeutic protocol, $1x10^5$ ASMCs were seeded in 6-well culture plates at a density of $1x10^5$ cells/well and allowed to attach for 20 hours. ASMCs were then incubated with CellTrace Violet solution (1:1000 in HBSS) for 20 minutes, followed by treatment with CSM (10-25%) for 4 hours. The CSM-containing medium was then removed and $1.5x10^5$ iPSC-MSCs were added into each well for a further 24 hours before the cells were harvested for analysis.

Trans-well co-culture of ASMCs and iPSC-MSCs

ASMCs were seeded in 6-well plates at a density of $1.x10^5$/well. iPSC-MSCs were seeded in a cell-culture insert with pores sized 0.4 μm (Falcon, Corning, NY, USA) at a density of $1.5x10^5$/well. ASMCs and iPSC-MSCs were incubated separately for 20 hrs to allow attachment overnight and then the inserts were transferred into the 6-well plates containing the ASMCs. ASMCs cultured in the presence of empty inserts were used as controls. After 20 hours of co-culture, the cells were treated with CSM (10-25%) for 4 hours, and the ASMCs were harvested for analysis.

Treatment of ASMCs with iPSC-MSC-conditioned medium

IPSC-MSC-conditioned medium (CdM) was prepared as previously described (9). Briefly, iPSC-MSCs were cultured in serum- and supplement-free DMEM for 24

hours. The supernatant was collected and concentrated 20-fold via centrifugation in ultra-filtration conical tubes (Amicon Ultra-15 with 5 kDa cut-off membranes). ASMCs were pre-treated with 20-fold diluted CdM for 4 hours. CSM was then added to the CdM at a final concentration of 10% or 25% and incubated for 4 hours before ASMCs were harvested for analysis. ASMCs in the control group were incubated with non-conditioned medium.

Detection of mitochondrial transfer in co-culture

To detect mitochondrial transfer in co-cultures of ASMCs and iPSC-MSCs, ASMCs were pre-stained with CellTrace Violet (Invitrogen), and iPSC-MSCs were pre-stained with MitoTracker Red (Invitrogen) for fluorescent microscopy or MitoTracker Green (Invitrogen) for flow cytometry, according to the manufacturer's instructions. Cells were mixed and seeded into 6-well plates at a density of $1x10^5$ ASMCs and $1.5x10^5$ iPSC-MSCs per well. 20 hours later, cells were treated with CSM (10-50%) and analyzed by flow cytometry. The percentage of MitoTracker-positive ASMCs was subsequently determined. For fluorescent microscopy, cells were fixed using 3.7% formaldehyde (Sigma-Aldrich, Dorset, UK) for 10 minutes, permeabilized in 0.1% Triton X-100 (Sigma-Aldrich) for 5 minutes and stained by Alexa Fluor 488-conjugated phalloidin (Invitrogen) in PBS with 1% BSA. The cells were then visualized using an inverted fluorescent microscope.

Mitochondrial ROS

Changes in mitochondrial ROS levels were assessed by staining with MitoSOX Red Mitochondrial Superoxide Indicator (Invitrogen). In the *in vitro* study, cells in 6-well

plates were washed with modified Hank's Balanced Salt Solution (HBSS) (containing Ca/Mg) (Sigma-Aldrich), and incubated with 5 μM MitoSOX diluted in modified HBSS for 30 minutes. The cells were then washed with HBSS without Ca/Mg (Sigma-Aldrich) and detached by incubation with Accutase (Sigma-Aldrich) for up to 5 min at 37 °C and 5% CO2. Cells were pelleted, re-suspended in HBSS and the median intensity of red fluorescence was determined using a FACSCanto II flow cytometer (BD Biosciences). For the *in vivo* study, intact mitochondria isolated from mouse lungs were incubated with 5 μM MitoSOX in 96-well plates for 30 minutes at 37°C. Fluorescence was measured at 510/580 nm using a fluorescence plate reader.

Mitochondrial membrane potential

Changes in mitochondrial membrane potential (ΔΨm) were determined by staining with JC-1 dye (Invitrogen). ASMCs or intact mitochondria from mouse lungs were incubated with 2 μM of JC-1 for 30 minutes at 37°C. The fluorescent signal was determined either using a FACSCanto II flow cytometer (BD Biosciences) for cells, or a fluorescence plate reader (Synergy HT Biotek, Winooski, VT, USA) for the isolated mouse mitochondria. Green fluorescence was measured at excitation/emission ratios of 485/535 nm and red fluorescence at 560/595 nm, and the ratio of red/green fluorescence was determined.

Annexin V staining

Apoptosis in cultured cells was detected by Annexin V staining. Briefly, cells were harvested, re-suspended at a density of $1x10^6$ cells/ml in assay buffer, incubated with

20-fold-diluted FITC-conjugated Annexin V solution (Invitrogen) for 15 minutes and analysed by flow cytometry.

Ozone-exposed mouse model

Experiments were performed under a Project License from the British Home Office, UK, under the Animals (Scientific Procedures) Act 1986. Male C57BL/6 mice were exposed to ozone at a concentration of 3 ppm for 3 hours using an ozonizer (model 500 Ozoniser, Sander, Wuppertal, Germany). Control mice were exposed to ambient air. $1x10^6$ iPSC-MSCs or PBS were administrated to mice by intravenous injection through the tail vein. The administration was performed either 24 hours prior (prophylactic protocol) or 6 hours after the exposure (therapeutic protocol). The treatment groups were as follows: Air/saline, Air with iPSC-MSCs administrated 24 hours prior-exposure (Air/-24hr), Ozone/saline, Ozone with iPSC-MSCs administrated 24 hours prior-exposure (Ozone/-24hr) and Ozone with iPSC-MSCs administrated 6 hour post-exposure (Ozone/+6hr).

Mice were anaesthetised for AHR measurements 21 hours after exposure. They were sacrificed immediately after the AHR measurements by intra-peritoneal injection of over-dosed pentobarbitone (100 mg/kg body weight). Bronchoalveolar lavage (BAL) was collected before the collection of the lungs. The right lobes were frozen for mitochondria extraction while left lobe was inflated with and fixed in paraformaldehyde. The larger lobe of the fixed lungs were later embedded into paraffin blocks and sectioned into 5 μm-sections.

Airway hyper-responsiveness (AHR) in mice

AHR was measured as previously described (10). Mice were anaesthetised by intra-peritoneal injection of ketamine/xylazine/saline mixture. The trachea was opened and inserted with a catheter through which the mouse was ventilated (MiniVent type 845, Hugo Sach Electronic, Germany) at 250 breaths/minute and a tidal volume of 250 µl. The animal was continuously monitored in a whole body plethysmograph (EMMS, Hants, UK). Pulmonary resistance (R_L) was recorded for 3 minute periods during increasing concentrations (4-256 mg/ml) of acetylcholine in PBS. Baseline R_L was defined as the R_L with nebulised PBS. A concentration-response curve was plotted for each animal and the concentration of acetylcholine that induced 100% elevation of R_L from baseline was derived (PC_{100}). The value of -log PC_{100} was taken as a measurement of AHR.

Measurement of cells and cytokines in BAL of mice

Bronchoalveolar lavage (BAL) was collected by rinsing the lungs three times with 0.8 ml PBS through an endotracheal tube. After centrifugation at 3000 rpm, 4°C for 5 min, the supernatant was collected as BAL fluid (BALF) while the cell pellets were resuspended in 200 µl PBS and counted on a haemocytometer for total cell number. BAL cell samples were centrifuged onto glass slides at 30g for 6 minutes (Shandon Cytospin 4; Thermo Electron Corporation, Waltham, MA, US). The resulting cell slides were air-dried overnight and stained using Diff-Quick kit (Reagena, Toivala, Finland) according to manufacturer's instructions. Differential count of white blood cells (neutrophil, macrophage, lymphocyte and eosinophil) was performed under an optical microscope (Olympus BH2, Olympus).

Isolation of intact mitochondria from mouse lungs

Intact mitochondria were isolated from mouse lungs using a Mitochondria Isolation Kit for Tissue (Thermo Fisher Scientific) and a Dounce tissue grinder set (Sigma) following the manufacturer's instructions. In brief, approximately 20 mg of lung tissue was washed with PBS supplemented with EDTA-free protease inhibitors (Roche). The tissue was homogenized with 5 strokes of Douncer A followed by 20 strokes of Douncer B in the corresponding reagent. The homogenates were centrifuged firstly at 700xg for 10 minutes at 4°C, to sediment large organelle fractions. The supernatants were centrifuged at 12,000xg for 5 minutes. The supernatants and pellets were collected as cytosolic fractions and mitochondrial fractions, respectively.

Detection of apoptosis in mouse lungs

Apoptosis in mouse lung sections were determined via TUNEL assay using the In Situ Cell Death Detection Kit, POD (Roche Applied Science, Mannheim, Germany). Lung sections were serially re-hydrated and antigen- retrieved in Sodium Citrate Buffer (10 mM sodium citrate, 0.05% Tween 20, pH 6.0) by heating in a microwave oven for 5 minutes. They were then washed with PBS and incubated with TUNEL reaction mixture for 1 hour. Lung sections were then washed and mounted in mounting medium (ProLong Gold antifade reagent with DAPI, Invitrogen) containing 4,6-diamidino-2-phenylindole (DAPI). Images of 5 random fields for each slide were captured at 20x magnification by a motorized inverted microscope (Olympus) and analysed using AxioVision (Zeiss).

References

1. Michaeloudes C, Sukkar MB, Khorasani NM, Bhavsar PK, Chung KF. TGF-beta regulates Nox4, MnSOD and catalase expression, and IL-6 release in airway smooth muscle cells. *American journal of physiology Lung cellular and molecular physiology* 2011; 300: L295-304.
2. Lian Q, Zhang Y, Zhang J, Zhang HK, Wu X, Lam FF, Kang S, Xia JC, Lai WH, Au KW, Chow YY, Siu CW, Lee CN, Tse HF. Functional mesenchymal stem cells derived from human induced pluripotent stem cells attenuate limb ischemia in mice. *Circulation* 2010; 121: 1113-1123.
3. Lau WK, Chan SC, Law AC, Ip MS, Mak JC. The role of MAPK and Nrf2 pathways in ketanserin-elicited attenuation of cigarette smoke-induced IL-8 production in human bronchial epithelial cells. *Toxicol Sci* 2012; 125: 569-577.
4. Walters, M.J., et al., *Cigarette smoke activates human monocytes by an oxidant-AP-1 signaling pathway: implications for steroid resistance.* Mol Pharmacol, 2005. **68**(5): p. 1343-53.
5. Oltmanns, U., et al., *Fluticasone, but not salmeterol, reduces cigarette smoke-induced production of interleukin-8 in human airway smooth muscle.* Pulm Pharmacol Ther, 2008. **21**(2): p. 292-7.
6. Li, X., et al., *Mitochondrial transfer of induced pluripotent stem cell-derived mesenchymal stem cells to airway epithelial cells attenuates cigarette smoke-induced damage.* Am J Respir Cell Mol Biol, 2014. **51**(3): p. 455-65.
7. Mitani, A., et al., *Restoration of Corticosteroid Sensitivity in Chronic Obstructive Pulmonary Disease by Inhibition of Mammalian Target of Rapamycin.* Am J Respir Crit Care Med, 2016. **193**(2): p. 143-53.
8. Aravamudan, B., et al., *Cigarette smoke-induced mitochondrial fragmentation and dysfunction in human airway smooth muscle.* Am J Physiol Lung Cell Mol Physiol, 2014. **306**(9): p. L840-54.
9. Zhang Y, Liao S, Yang M, Liang X, Poon MW, Wong CY, Wang J, Zhou Z, Cheong SK, Lee CN, Tse HF, Lian Q. Improved cell survival and paracrine capacity of human embryonic stem cell-derived mesenchymal stem cells promote

therapeutic potential for pulmonary arterial hypertension. *Cell Transplant* 2012; 21: 2225-2239.

10. Wiegman CH, Li F, Clarke CJ, Jazrawi E, Kirkham P, Barnes PJ, Adcock IM, Chung KF. A comprehensive analysis of oxidative stress in the ozone-induced lung inflammation mouse model. *Clinical science* 2014; 126: 425-440.